mM stock solutions. BIS-1 and CHE were dissolved in dimethyl sulfoxide (DMSO, Sigma) to yield stock solutions of 200 μM and 5 mM, respectively. Phosphatidylinositol 4,5-bisphosphate ($PIP_2$; Calbiochem, San Diego, CA, USA) was directly dissolved in the control pipette solution at a concentration of 50 μM with 30 min sonication on ice. In a subset of experiments, the cells were pre-incubated with 5 μg/ml PTX (Seikagaku, Japan) for at least 2 h to inhibit a PTX-sensitive G protein, as previously described [16].

### Electrophysiological recordings and data analysis

The cells attached to glass coverslips were transferred to a 0.5-ml recording chamber perfused with extracellular solution at 1–2 ml/min after 48 h of transfection. The chamber was mounted on the stage of an inverted microscope (ECLIPSE TE2000-U; Nikon, Tokyo, Japan) and maintained at 25°C. Patch-clamp experiments were conducted on GFP-positive cells. Whole-cell membrane currents were recorded with an EPC-8 patch-clamp amplifier (HEKA, Lambrecht, Germany), and data were low-pass filtered at 1 kHz, acquired at 5 kHz through an LIH-1600 analog-to-digital converter (HEKA) and stored on a hard disc drive, using the PulseFit software program (HEKA). Patch pipettes were fabricated from borosilicate glass capillaries (Narishige, Japan) using a horizontal microelectrode puller (P-97; Sutter Instrument Co., USA), and the tips were then fire-polished using a microforge. Patch pipettes had a resistance of 2.5–4.0 MΩ when filled with the pipette solution. Membrane currents were measured at a holding potential of −40 mV or during the voltage ramp protocol ($dV/dt$=±0.4 V/s), which consisted of an ascending (depolarizing) phase from the holding potential to +50 mV followed by a descending (hyperpolarizing) phase to −130 mV. The current–voltage ($I$–$V$) relationship was determined during descending phase.

All of the averaged data are expressed as the mean ± SEM, with the number of experiments shown in parentheses. Statistical comparisons were analyzed using either Student's unpaired $t$ test or ANOVA followed by Dunnett's *post hoc*, as appropriate. Differences were considered to be statistically significant if a value of $P<0.05$ was obtained.

## Results

### The nature of $I_{GIRK}$ during exposure to ATP in CHO cells expressing $P2Y_1$ receptor

The effect of extracellular ATP on $I_{GIRK}$ was examined in cells transfected with $P2Y_1$ receptor by measuring whole-cell membrane currents at a holding potential of −40 mV and during hyperpolarizing voltage ramps from +50 to −130 mV. The bath application of 10 μM ATP initially evoked a rapid outward shift of the holding current ($I_{GIRK}$ activation), which then progressively declined to the baseline level within ~1–2 min (a subsequent inward shift, Fig. 1a) despite the continued presence of the agonist.

Figure 1b illustrates the membrane currents during hyperpolarizing voltage ramps, recorded before and during application of ATP. The membrane current was calculated by digital subtraction of the current traces under control conditions from that shortly after ATP application and showed an inward rectification (Fig. 1c). $I_{K,ACh}$ is activated by a membrane-delimited pathway involving a PTX-sensitive G protein ($G_{i/o}$) in guinea-pig atrial myocytes [24]. The present experiment also found that pre-exposure to 5 μg/ml PTX for 2 h abolished the action of extracellular ATP (Fig. 1d), suggesting that a PTX-sensitive G protein mediates the activation of $I_{GIRK}$ by $P2Y_1$ receptor stimulation.

The functional regulation of $P2Y_1$ receptor was further analyzed using 10 μM ACh to induce an activation of $I_{GIRK}$ at −40 mV (Fig. 2a). The further addition of ATP initially had an additive effect on ACh-activated $I_{GIRK}$ but then markedly inhibited the current (Fig. 2a; the number of cells

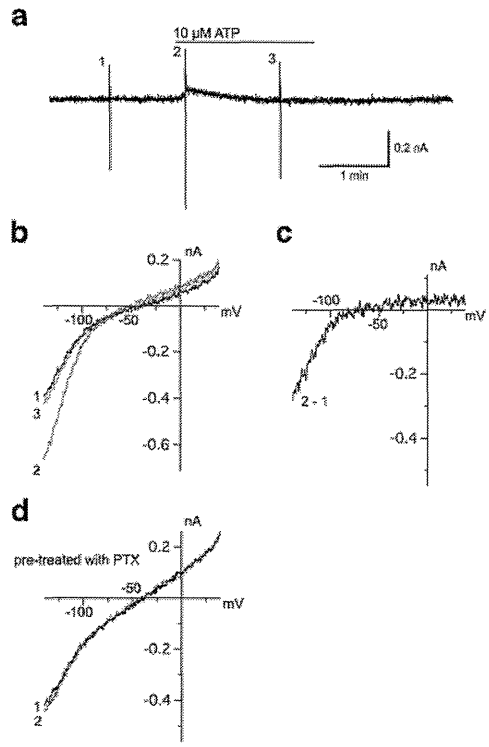


**Fig. 1** Effect of ATP on the activation of $I_{GIRK}$ in CHO cells transfected with $P2Y_1$ receptor. **a** The whole-cell currents recorded at a holding potential of −40 mV and during exposure to 10 μM ATP. **b** Superimposed $I$–$V$ relationships measured during the voltage ramps applied at the points indicated by numbers (*1–3*) in panel (**a**). **c** $I$–$V$ relationship obtained by digital subtraction of current traces as indicated. **d** After pretreatment with 5 μg/ml PTX for 2 h, the $I$–$V$ relationships were measured during the voltage ramps

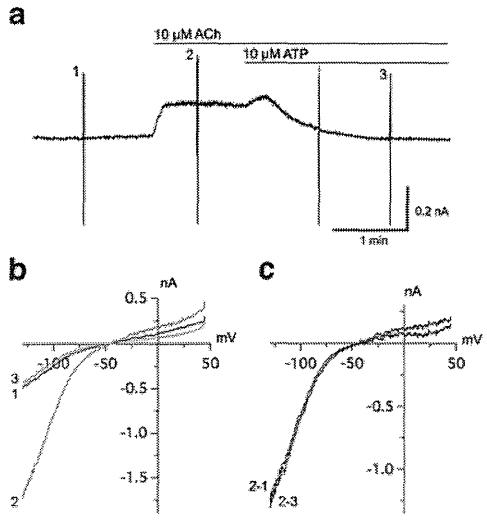


**Fig. 2** Inhibition of ACh-activated $I_{GIRK}$ by ATP. **a** The whole-cell currents recorded at a holding potential of −40 mV and during voltage ramps applied before (*1*), during exposure to 10 μM ACh (*2*), and after further addition of 10 μM ATP (*3*). **b** Superimposed *I–V* relationships measured during the voltage ramps applied at the points indicated by numerals (*1–3*) in panel (**a**). **c** Superimposed *I–V* relationships for the difference currents obtained by digital subtraction of current records as indicated. The voltage ramp traces were truncated for the purpose of presentation

positively responded to ATP was 18/19). The ACh-activated maximal $I_{GIRK}$ was decreased by 92.44±10.61% ($n$=19), when measured 3 min after application of 10 μM ATP, which indicates that external ATP almost inhibited the ACh-activated $I_{GIRK}$. Figure 2b and c show that the ACh-activated $I_{GIRK}$ current also exhibited an inwardly rectifying *I–V* relationship, which is consistent with the properties of $I_{K,ACh}$ in guinea-pig atrial myocytes. In addition, $I_{GIRK}$ isolated by digital subtraction of the currents in the presence of ACh from that after ATP application also exhibited an inwardly rectifying *I–V* relationship.

In different sets of experiments, we examined the background currents and the expression ability of our CHO cell expression system. The results show that bath application of ACh and ATP could not induce any discernible currents in non-transfected cells (Fig. S1a) and in cells transfected only with GFP + GIRK1/GIRK4 (Fig. S1b). However, ACh evoked persistent $I_{GIRK}$ currents in cells transfected with GFP + GIRK1/GIRK4 + $M_2$ (Fig. S1c), which was consistently inhibited by ATP when co-transfected with $P2Y_1$ in addition to GIRK subunits and $M_2$ (Fig. S1d). Figure S1e shows the representative image of the cells showing GFP expression. On the other hand, the inhibition of $I_{GIRK}$ currents was not observed in cells without $P2Y_1$ transfection (Fig. S1c). These results indicate that functional expression of intrinsic P2Y and $M_2$ receptors was almost null in our CHO cell expression system, and all plasmids were successfully expressed in our cells. To exclude the possibility that the activation of $I_{GIRK}$ was affected by G protein-coupled receptor–G protein interaction, we observed the effects of ATP on ACh-activated $I_{GIRK}$ in CHO cells co-transfected lower doses (0.2–0.5 μg) of $P2Y_1$ together with 0.5 μg GFP +1 μg GIRK1/GIRK4+1 μg $M_2$. Figure S1f shows that the inhibition of ACh-activated $I_{GIRK}$ by ATP in cells co-transfected with 0.2 μg $P2Y_1$ is almost the same as that co-transfected with 1 μg $P2Y_1$.

## The modulation of $RGS_2$ on ATP-induced inhibition of $I_{GIRK}$

Regulators of G-protein signaling (RGS) proteins modulate the signal transduction via G protein-coupled receptors (GPCR). These proteins enhance GTP hydrolysis by accelerating the intrinsic GTPase activity of Gα-subunit, and thereby terminate the G protein activation cycle [4, 31, 39]. $RGS_2$ (one of the important inhibitor of $G_q\alpha$ subunit) was co-transfected with GIRK1/GIRK4, $M_2$ and $P2Y_1$ cDNAs to explore the inhibitory mechanism of ATP on $I_{GIRK}$. Figure 3a shows that the inhibitory action of ATP on ACh-activated $I_{GIRK}$ was significantly attenuated with the co-expression of $RGS_2$. Figure 3c shows that the inhibitory degree of the ACh-activated $I_{GIRK}$ was only 50.7± 9.1% ($n$=15) 3 min after exposure to 10 μM ATP, which

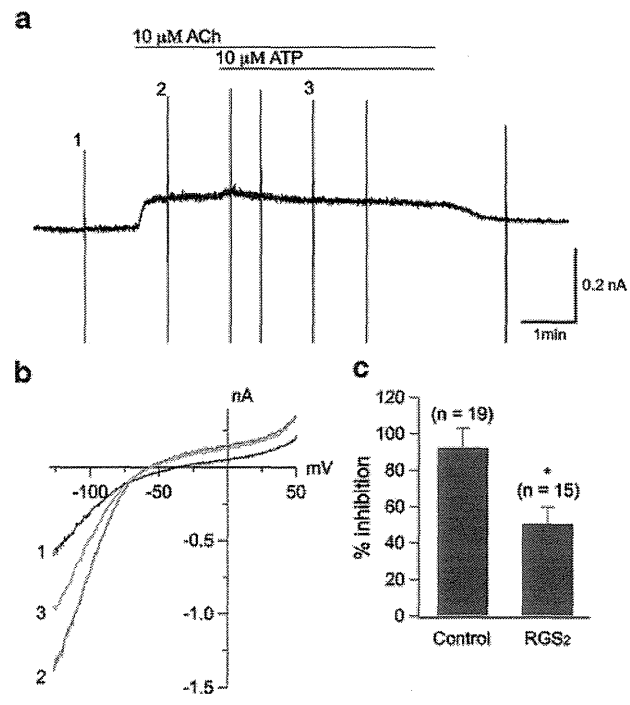


**Fig. 3** The modulation of $RGS_2$ on the ATP-induced inhibition of $I_{GIRK}$. **a** Whole-cell currents recorded in CHO cell co-transfected with $RGS_2$ at a holding potential of −40 mV. **b** Superimposed *I–V* relationships measured during the voltage ramps applied at the points indicated by numerals (*1–3*) in panel (**a**). **c** ATP-induced inhibition of $I_{GIRK}$ (*$P$<0.05 vs. control)

is significantly ($P<0.05$) lower than that of control (92.44±10.61%, $n=19$). Therefore, the activation of $G_q$ protein is involved in the ATP-induced inhibition of $I_{GIRK}$. Besides, our supplementary experiment data observed in CHO cells co-transfected 1 μg $M_1$ receptor (coupled with $G_q$) together with 0.5 μg GFP+1 μg GIRK1+1 μg GIRK4+1 μg $M_2$ (Fig. S3a) also supports the result that the activation of $G_q$ protein is involved in the agonist-induced inhibition of $I_{GIRK}$ in this experiment.

In order to further confirm the result that co-expression of $RGS_2$ led to the inhibition of the signal transduction via $G_q$ protein-coupled receptors in our cell expression system, we co-transfected GFP + GIRK1/GIRK4+$M_2$+$RGS_2$ together with $\alpha_1$-adrenergic receptor that has been generally accepted to be coupled to $G_q$ [8]. Similar to the inhibition of ACh-activated $I_{GIRK}$ currents by ATP, bath application of PHE (a selective $\alpha_1$ receptor agonist, 30 μM) significantly inhibited the ACh-activated $I_{GIRK}$ currents by 94.8±10.1% ($n=7$) in cells co-expressing $\alpha_1$ receptor (Fig. S2a), whereas only by 40.3±5.4% ($n=5$, $P<0.01$) in cells co-expressing $RGS_2$+$\alpha_1$ receptor (Fig. S2b), implicating that the attenuation of $I_{GIRK}$ inhibition by ATP in cells co-expressing $RGS_2$ is involved in blockade of $G_q$ protein in our experiment.

## Role of membrane $PIP_2$ in ATP-induced decline of $I_{GIRK}$

A previous study indicated that ATP receptor stimulation could inhibit the $I_{K,ACh}$ channels through depletion of membrane $PIP_2$ in guinea pig atrium [44]. PI4P-5K (the enzyme that catalyzes $PIP_2$ synthesis [11]) was co-expressed with GIRK1/GIRK4, $M_2$, and $P2Y_1$ cDNAs. Figure 4a shows that the co-expression of PI4P-5K markedly ($P<0.01$) prevented the inhibitory action of ATP on ACh-activated $I_{GIRK}$, compared with that in control (55.2±10.0%, $n=13$ vs. 92.44±10.61%, $n=19$; Fig. 4c). This result is consistent with the view that a characteristic progressive decline of $I_{GIRK}$ in the presence of extracellular ATP is mediated through the depletion of membrane $PIP_2$.

If the reduction in membrane $PIP_2$ underlies the decline of $I_{GIRK}$ during exposure to ATP, intracellular loading of exogenous $PIP_2$ may attenuate the inhibitory action of ATP on ACh-activated $I_{GIRK}$. As demonstrated in Fig. 5a and b, intracellular dialysis of 50 μM $PIP_2$ for 5–7 min through a recording pipette significantly reduced the inhibition degree of ACh-activated $I_{GIRK}$ by ATP. The inhibition of $I_{GIRK}$ (Fig. 5c) only reached 18.2±6.4% ($n=5$) 3 min after bath application of 10 μM ATP, which is markedly ($P<0.01$) lower than that of the control (92.44±10.61%, $n=19$). This result further indicates that the reduction in membrane $PIP_2$ is closely linked to the inhibitory action of ATP on $I_{GIRK}$.

PKC activation was previously reported to produce inhibitory action on $I_{K,ACh}$ [14, 22, 31, 35]. In our experiments, however, bath application of two different PKC

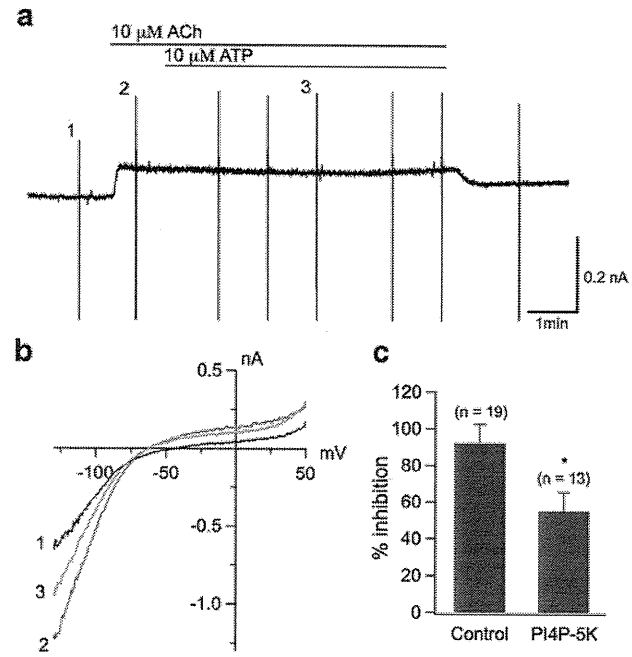


**Fig. 4** Co-expression of PI4P-5K attenuated the ATP-induced inhibition of $I_{GIRK}$. **a** The whole-cell currents recorded in CHO cell co-transfected with PI4P-5K in the presence of ACh and ATP at a holding potential of −40 mV. **b** Superimposed *I–V* relationships measured during the voltage ramps applied at the points indicated by numerals (*1–3*) in panel (**a**). **c** ATP-induced inhibition of $I_{GIRK}$ (*$P<0.05$ vs. control)

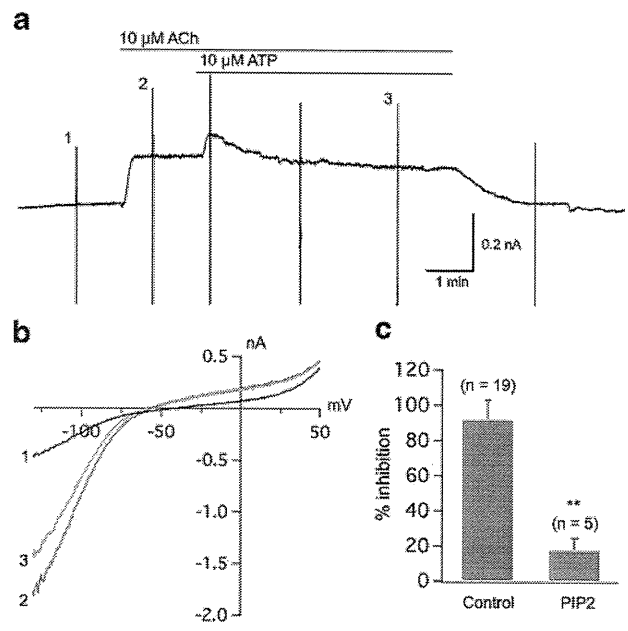


**Fig. 5** Effect of $PIP_2$ (intracellularly loaded) on the ATP-induced inhibition of $I_{GIRK}$. **a** Whole-cell currents recorded with $PIP_2$ intracellular dialysis for 5–7 min at a holding potential of −40 mV, and then in the presence of ACh and ATP. **b** Superimposed *I–V* relationships measured during the voltage ramps applied at the points indicated by numerals (*1–3*) in panel (**a**). **c** ATP-induced inhibition of $I_{GIRK}$ (**$P<0.01$ vs. control)

inhibitors, bisindolylmaleimide (BIS-1, 200 nM, Fig. 6a and b) and chelerythrine (CHE, 5 μM, Fig. 6b), did not significantly alter the inhibition degree of ACh-activated $I_{GIRK}$ by ATP (control, 92.44±10.61%, $n$=19; BIS-I, 95.7±15.0%, $n$=7; CHE, 92.3±17.5%, $n$=6), thus suggesting that PKC activation is not involved in the ATP-induced inhibition of $I_{GIRK}$ [7, 28].

## Effects of P2Y receptor subtype stimulation on $I_{GIRK}$

Different P2Y receptor subtpes, namely $P2Y_2$, $P2Y_4$, and $P2Y_{12}$, were respectively transfected together with GIRK1/GIRK4 channels to explore the effects of the P2Y receptor stimulation on $I_{GIRK}$. In the experiment, 10 μM UTP was used as an alternative to ATP to activate $P2Y_2$ and $P2Y_4$ receptors because it seems that these two receptors are more sensitive to UTP [38, 41]. Figure 7a shows the representative $I_{GIRK}$ traces elicited by stimulating $P2Y_2$, $P2Y_4$, and $P2Y_{12}$ receptors, respectively. The persistent $I_{GIRK}$ currents elicited by the stimulation of $P2Y_2$ or $P2Y_{12}$ receptor suggest that little membrane $PIP_2$ was depleted, whereas the current evoked by the stimulation of $P2Y_4$ receptor was transient, which suggests that depletion of membrane $PIP_2$ occurred. Figure 7b and c shows the amplitudes of $I_{GIRK}$ normalized to the peak amplitude one minute ($I_{1min}/I_{peak}$) and 3 min ($I_{3min}/I_{peak}$) after application of an agonist. The normalized amplitude of $I_{GIRK}$ for $P2Y_2$ or $P2Y_{12}$ was significantly ($P$<0.01) larger than that of $P2Y_1$ both 1 and 3 min after application of an agonist, whereas the amplitude of $I_{GIRK}$ for $P2Y_1$ or $P2Y_4$ 3 min after receptor stimulation was significantly ($P$<0.05) lower than that for the same receptor 1 min after receptor stimulation.

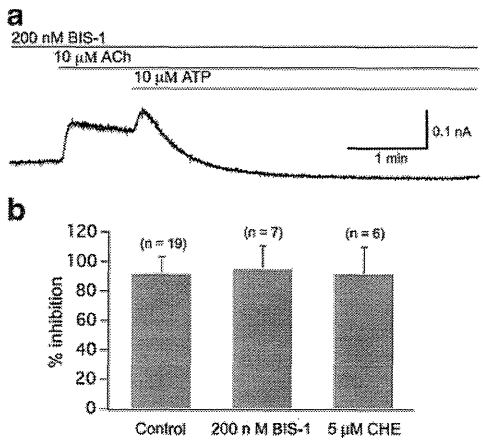


**Fig. 6** PKC inhibitors did not attenuate the ATP-induced inhibition of $I_{GIRK}$. **a** The whole-cell currents recorded in CHO cell pre-treated with 200 nM BIS-1 in the presence of ACh and ATP at a holding potential of −40 mV. **b** ATP-induced inhibition of $I_{GIRK}$ in the presence of 200 nM BIS-1 or 5 μM CHE

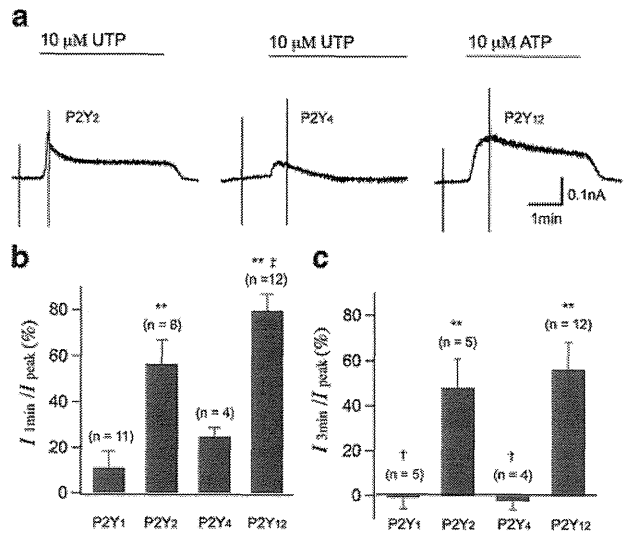


**Fig. 7** Comparison of $I_{GIRK}$ currents evoked by stimulating different P2Y receptor subtypes. **a** The whole-cell currents in CHO cells transfected with $P2Y_2$, $P2Y_4$, and $P2Y_{12}$ receptor subtypes at a holding potential of −40 mV. **b** Inhibition of $I_{GIRK}$ 1 min after stimulation of $P2Y_2$, $P2Y_4$, and $P2Y_{12}$ receptors. **c** Inhibition of $I_{GIRK}$ 3 min after stimulation of $P2Y_2$, $P2Y_4$, and $P2Y_{12}$ receptors (**$P$<0.01 vs. $P2Y_1$ or $P2Y_4$; ‡$P$<0.05 vs. $P2Y_2$; †$P$<0.05 vs. $I_{1min}/I_{peak}$)

Treatment with 10 μM ACh was first used to induce an $I_{GIRK}$ current at −40 mV, and then 10 μM UTP or ATP was employed to stimulate $P2Y_2$, $P2Y_4$, or $P2Y_{12}$ to further examine the effects of $P2Y_s$ receptor stimulation on ACh-activated $I_{GIRK}$. Figure 8a and b shows that the nature of the current evoked by stimulating $P2Y_4$ receptor with UTP was almost the same as that elicited by stimulating $P2Y_1$ (Fig. 2). The inhibitory degree of ACh-activated $I_{GIRK}$ by the stimulation of $P2Y_4$ was 99.6±22.5% ($n$=5), which was similar to that evoked by the stimulation of $P2Y_1$ receptor (Fig. 8c). Figure S3b and c shows that addition of an agonist (ATP or UTP) caused the ACh-activated $I_{GIRK}$ to increase further (there was 1/13 cell co-transfected with $P2Y_2$ that did not respond to UTP). The addition activation of $I_{GIRK}$ by the stimulation of $P2Y_2$ declined slightly, but still much higher than the ACh-activated $I_{GIRK}$ level 3 min after treatment with UTP (Fig. S3b). On the other hand, the addition activation of $I_{GIRK}$ by the stimulation of $P2Y_{12}$ almost did not decline (Fig. S3c).

## Discussion

The activation of $I_{K,ACh}$ is due to the activation of $G_{i/o}$ protein [34]. The rapid activation phase of $I_{K,ACh}$ evoked by exposure to ATP is caused by stimulation of P2Y receptor, leading to a membrane-delimited, $G_{i/o}$-mediated channel activation in guinea-pig atrial myocytes [14, 25, 44]. However, there is no consensus on the mechanism of $I_{K,ACh}$

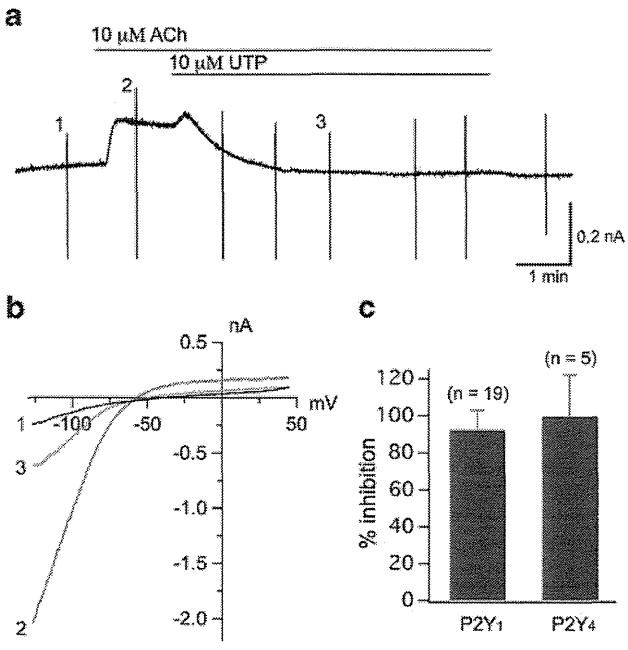


**Fig. 8** Effect of $P2Y_4$ stimulation on ACh-activated $I_{GIRK}$. **a** The whole-cell currents recorded at a holding potential of −40 mV, and in the presence of ACh and UTP. **b** Superimposed *I–V* relationships measured during the voltage ramps applied at the points indicated by numerals (*1–3*) in panel (**a**). **c** Inhibitory degree of $I_{GIRK}$ by the stimulation of $P2Y_1$ and $P2Y_4$ receptors

inhibition produced by agonists. Several groups [7, 14, 18, 25, 29, 44] reported that activation of PLC contributes to the inhibition of $I_{K,ACh}$ by decreasing membrane $PIP_2$. However, others [15, 23, 32, 36] suggest that the downstream activation of PKC underlies the inhibition of $I_{K,ACh}$. There are also some pieces of evidence to suggest that reduction in membrane $PIP_2$ and PKC activation are both involved in the $I_{K,ACh}$ inhibition by agonists such as carbachol [22] and ACh [17].

A previous study in the guinea-pig atrium indicated that the inhibition of $I_{K,ACh}$ by extracellular ATP is attenuated by blocking PLC activity with compound 48/80 and by exogenously adding $PIP_2$ in the atrial myocytes [44]. This observation suggests that the ATP-induced activation of PLC and the concomitant reduction of $PIP_2$ contribute to the inhibition of $I_{K,ACh}$ by ATP. In addition, $RGS_2$ protein is one of the important inhibitor of the $G_q\alpha$ subunit and terminates $G_q$ signaling through its GTPase-activating protein mechanism [4, 31, 39]. The present experiment found that co-expression of $RGS_2$ significantly reduced the ATP-induced inhibition of $I_{GIRK}$, thus confirming the view that the inhibition of $I_{GIRK}$ by ATP is mediated through the $G_q$ protein-coupled P2Y receptors in native cardiac myocytes [14, 25]. The present study also demonstrated that the ATP-induced inhibition of $I_{GIRK}$ is markedly attenuated by both co-expression of PI4P-5K and intracellular dialysis with $PIP_2$ in CHO cells. These data are consistent with a previous study in guinea-pig atrial myocytes [44] and support the view that a decrease in membrane $PIP_2$ is closely linked to the ATP-induced inhibition of $I_{K,ACh}$. In contrast to the study of Keselman et al. [17], however, the PKC inhibitor BIS-1 and CHE did not alter the inhibition of ATP on ACh-activated $I_{GIRK}$, thus indicating PKC activation might not be involved in the inhibition of $I_{GIRK}$ by ATP [9, 28]. Taken together, the current data fully support the hypothesis that the reduction in membrane $PIP_2$ via activation of $G_q$-PLC is mainly responsible for the inhibition of $I_{K,ACh}$ channels by externally applying ATP.

Previous reports have indicated that $P2Y_1$, $P2Y_2$, and $P2Y_4$ receptor subtypes are coupled to PTX-insensitive $G_q$ proteins that activate PLC and then produce a fall in membrane $PIP_2$ levels, whereas $P2Y_{12}$ receptor is only coupled to PTX-sensitive $G_{i/o}$ protein to inhibition of adenylate cyclase [1, 9, 37, 41]. However, the coupling to signaling transduction pathways appears to be much more complex. An example is that the $G_q$-coupled $P2Y_1$ receptor, known to inhibit GIRK channels, efficiently activates GIRK1/GIRK2 channels in cultured rat sympathetic neurons [12]. A sequence analysis also indicates that the two regions (the third intracellular loop and the C-terminal tail), implicated in G protein specificity, vary greatly among the P2Y receptor subtypes [40]. The present study found that the stimulation of $P2Y_1$ or $P2Y_4$ receptor evoked a transient activation of $I_{GIRK}$ followed by a persistent inhibition (Figs. 1a and 7a), thus suggesting that a large amount of membrane $PIP_2$ was consumed via activation of $G_q$-PLC pathway. This result might implicate that the two receptors are mainly coupled to $G_q$ protein. Contrary to previous reports [1, 9, 37, 41], however, the activation phase of $I_{GIRK}$ evoked by the stimulation of these two receptors reflects the existence of $G_{i/o}$ coupling although it might be relatively weak. In contrast, the stimulation of $P2Y_2$ or $P2Y_{12}$ receptor induced a persistent activation of $I_{GIRK}$ (Fig. 7a), indicating that little membrane $PIP_2$ was consumed and resultantly implicating that these two receptors are mainly coupled to $G_{i/o}$ protein. Bodor and colleagues have found that purified $P2Y_{12}$ receptor can form a functional receptor when reconstituted with $G_i$ protein, but not when reconstituted with $G_q$ protein [6]. This is consistent with the present finding that the $P2Y_{12}$ receptor is coupled to $G_{i/o}$ protein to activate $I_{GIRK}$. In addition, the decay $I_{GIRK}$ evoked by the stimulation of $P2Y_2$ was relatively rapid in comparison to the $P2Y_{12}$, suggesting that some amount of membrane $PIP_2$ was still consumed during the stimulation of $P2Y_2$ and resultantly implicating that $P2Y_2$ is also weakly coupled to $G_q$ protein. The $P2Y_2$ receptor is generally classified to the (PTX-resistant) $G_q$-coupled subfamily [9, 19, 41]. However, the data in the present study suggested that $P2Y_2$ is also coupled to $G_{i/o}$ protein as suggested by other researchers [37], though they

believed that $P2Y_2$ receptor primarily mediates its function through coupling to $G_q$. Furthermore, these data are also supported by the fact that $P2Y_2$ receptor is sensitive to PTX in stable expressed astrocytoma cells [33] and in human erythroleukemia cells [2].

There is an abundant expression of $P2Y_2$ mRNA in both human atria and ventricles, whereas the mRNA level of $P2Y_2$ is lower than that of $P2Y_1$ or $P2Y_4$ in mouse cardiomyocytes [43]. Musa and colleagues [30] have also indicated that the $P2Y_2$ mRNA level is the most abundant of the eight P2Y receptors in the human right atrium, but is lower than $P2Y_1$ in human sinoatrial node (SAN). They also found that the distribution of P2Y receptor subtypes in rat right atrium, left ventricle, and SAN is quite different with those in the human heart. These results indicate that the P2Y receptor expression varies greatly in the heart, implicating that responses to the stimulation of P2Y receptor are also diverse in different types of cardiac cells. The current study may contribute to understanding the precise regulatory mechanisms underlying the cardiac signaling pathway mediated by P2Y receptors.

**Acknowledgements** This study was supported by grants (No. 22590205 and No. 22590206) from the Ministry of Education, Science, and Culture of Japan; the Uehara Memorial Foundation; and health science research grants from the Ministry of Health, Labor and Welfare of Japan for Clinical Research on Measures for Intractable Diseases.

**Ethical standards** The authors declare that the experiment comply with the current laws of Japan.

**Conflict of interest** The authors declare that they have no conflict of interest.

## References

1. Abbracchio MP, Burnstock G, Boeynaems JM, Barnard EA, Boyer JL, Kennedy C, Knight GE, Fumagalli M, Gachet C, Jacobson KA, Weisman GA (2006) International Union of Pharmacology LVIII: update on the P2Y G protein-coupled nucleotide receptors: from molecular mechanisms and pathophysiology to therapy. Pharmacol Rev 58:281–341
2. Baltensperger K, Porzig H (1997) The $P_{2U}$ purinoceptor obligatorily engages the heterotrimeric G protein $G_{16}$ to mobilize intracellular $Ca^{2+}$ in human erythroleukemia cells. J Biol Chem 272:10151–10159
3. Banfi C, Ferrario S, De Vincenti O, Ceruti S, Fumagalli M, Mazzola A, D'Ambrosi N, Volonte C, Fratto P, Vitali E, Burnstock G, Beltrami E, Parolari A, Polvani G, Biglioli P, Tremoi E, Abbracchio MP (2005) P2 receptors in human heart: upregulation of P2X6 in patients undergoing heart transplantation, interaction with TNFalpha and potential role in myocardial cell death. J Mol Cell Cardiol 39:929–939
4. Bernstein LS, Ramineni S, Hague C, Cladman W, Chidiac P, Levey AL, Hepler JR (2004) RGS2 binds directly and selectively to the M1 muscarinic acetylcholine receptor third intracellular loop to modulate Gq/11alpha signaling. J Biol Chem 279:21248–21256
5. Birnbaumer L (2007) Expansion of signal transduction by G proteins. The second 15 years or so: from 3 to 16 $\alpha$ subunits plus $\beta\gamma$ *dimmers. Biochim Biophys Acta 1768:772–793*
6. Bodor ET, Waldo GL, Hooks SB, Corbitt J, Boyer JL, Harden TK (2003) Purification and functional reconstitution of the human $P2Y_{12}$ receptor. Mol Pharmacol 64:1210–1216
7. Cho H, Lee D, Lee SH, Ho WK (2005) Receptor-induced depletion of phosphatidylinositol 4,5-bisphosphate inhibits inwardly rectifying $K^+$ channels in a receptor-specific manner. Proc Natl Acad Sci USA 102:4643–4648
8. Docherty JR (2010) Subtypes of functional alpha1-adrenoceptor. Cell Mol Life Sci 67:405–417
9. Erb L, Liao Z, Seye CI, Weisman GA (2006) P2 receptors: intracellular signaling. Pflugers Arch 452:552–562
10. Erlinge D, Burnstock G (2008) P2 receptors in cardiovascular regulation and disease. Purinergic Signalling 4:1–20
11. Falkenburger BH, Jensen JB, Hille B (2010) Kinetics of PIP2 metabolism and KCNQ2/3 channel regulation studied with a voltage-sensitive phosphatase in living cells. J Gen Physiol 135:99–114
12. Filippov AK, Fernandez-Fernandex JM, Marsh SJ, Simon J, Barnard EA, Brown DA (2004) Activation and inhibition of neuronal G protein-gated inwardly rectifying K(+) channels by P2Y nucleotide receptors. Mol Pharmacol 66:468–477
13. Friel DD, Bean BP (1990) Dual control by ATP and acetylcholine of inwardly rectifying $K^+$ channels in bovine atrial cells. Pflugers Arch 415:651–657
14. Hara Y, Nakaya H (1997) Dual effects of extracellular ATP on the muscarinic acetylcholine receptor-operated $K^+$ current in guinea-pig atrial cells. Eur J Pharmacol 324:295–303
15. Hill JJ, Peralta EG (2001) Inhibition of a $G_i$-activated potassium channel (GIRK1/4) by the $G_q$-coupled m1 muscarinic acetylcholine receptor. J Biol Chem 276:5505–5510
16. Hwang TC, Horie M, Nairn AC, Gadsby DC (1992) Role of GTP-binding proteins in the regulation of mammalian cardiac chloride conductance. J Gen Physiol 99:465–489
17. Keselman I, Fribourg M, Felsenfeld DP, Logothetis DE (2007) Mechanism of PLC-mediated Kir3 current inhibition. Channels (Austin) 1:113–123
18. Kobrinsky E, Mirshahi T, Zhang H, Jin T, Logothetis DE (2000) Receptor-mediated hydrolysis of plasma membrane messenger PIP2 leads to $K^+$-current desensitization. Nat Cell Biol 2:507–514
19. Koles L, Gerevich Z, Oliveira JF, Zadori ZS, Wirkner K, Illes P (2008) Interaction of P2 purinergic receptors with cellular macromolecules. Naunyn-Schmiedeberg's Arch Pharmacol 377:1–33
20. Krapivinsky G, Gordon EA, Wickman K, Velimirovic B, Krapivinsky L, Clapham DE (1995) The G-protein-gated atrial $K^+$ channel $I_{KACh}$ is a heteromultimer of two inwardly rectifying $K^+$-channel proteins. Nature 374:135–141
21. Kurachi Y, Nakajima T, Sugimoto T (1986) On the mechanism of activation of muscarinic $K^+$ channels by adenosine in isolated atrial cells: involvement of GTP-binding proteins. Pflugers Arch 407:264–274
22. Leaney JL, Dekker LV, Tinker A (2001) Regulation of a G protein-gated inwardly rectifying $K^+$ channel by a $Ca^{2+}$-independent protein kinase C. J Physiol 534:367–379
23. Mao J, Wang X, Chen F, Wang R, Rojas A, Shi Y, Piao H, Jiang C (2004) Molecular basis for the inhibition of G protein-coupled inward rectifier $K^+$ channels by protein kinase C. Proc Natl Acad Sci USA 101:1087–1092
24. Matsuura H, Sakaguchi M, Tsuruhara Y, Ehara T (1996) Activation of the muscarinic $K^+$ channel by $P_2$-purinoceptors via pertussis toxin-sensitive G proteins in guinea-pig atrial cells. J Physiol 490:659–671

25. Matsuura H, Ehara T (1996) Modulation of the muscarinic $K^+$ channel by $P_2$-purinoceptors in guinea-pig atrial myocytes. J Physiol 497:379–393
26. Matsuura H, Ehara T (1992) Activation of chloride current by purinergic stimulation in guinea pig heart cells. Circ Res 70:851–855
27. Matsuura H, Ehara T (1997) Selective enhancement of the slow component of delayed rectified $K^+$ current in guinea-pig atrial cells by external ATP. J Physiol 503:45–54
28. Matsuura H, Tsuruara Y, Sakaguchi M, Ehara T (1996) Enhancement of delayed rectifier $K^+$ current by $P_2$-purinoceptor stimulation in guinea-pig atrial. J Physiol 490:647–658
29. Meyer T, Wellner-Kienitz MC, Biewald A, Bender K, Eickel A, PottlT L (2001) Depletion of phosphatidylinositol 4,5-bisphosphate by activation of phospholipase C-coupled receptors causes slow inhibition but not desensitization of G protein-gated inward rectifier $K^+$ current in atrial myocytes. J Biol Chem 276:5650–5658
30. Musa H, Tellez JO, Chandler NJ, Greener ID, Maczewski M, Mackiewicz U, Beresewicz A, Molenaar P, Boyett MR, Dobrzynski H (2009) P2 purinergic receptor mRNA in rat and human sinoatrial node and other heart regions. Naunyn Schmiedebergs Arch Pharmacol 379:541–549
31. Neitzel KL, Hepler JR (2006) Cellular mechanisms that determine selective RGS protein regulation of G protein-coupled receptor signaling. Semin Cell Dev Biol 17:383–389
32. Nikolov EN, Ivanova-Nikolova TT (2004) Coordination of membrane excitability through a GIRK1 signaling complex in the atria. J Biol Chem 279:23630–23636
33. Parr CE, Sullivan DM, Paradiso AM, Lazarowski ER, Burch LH, Olsen JC, Erb L, Weisman GA, Boucher RC, Turner JT (1994) Cloning and expression of a human $P_{2U}$ nucleotide receptor, a target for cystic fibrosis pharmacotherapy. Proc Natl Acad Sci USA 91:3275–3279
34. Pfaffinger PJ, Martin JM, Hunter DD, Nathanson NM, Hille B (1985) GTP-binding proteins couple cardiac muscarinic receptors to a K channel. Nature 317:536–538
35. Soejima M, Noma A (1984) Mode of regulation of the ACh-sensitive K-channel by the muscarinic receptor in rabbit atrial cells. Pflugers Arch 400:424–431
36. Stevens EB, Shah BS, Pinnock RD, Lee K (1999) Bombesin receptors inhibit G protein-coupled inwardly rectifying $K^+$ channels expressed in *Xenopus* oocytes through a protein kinase C-dependent pathway. Mol Pharmacol 55:1020–1027
37. Talasila A, Germack R, Dickenson JM (2009) Characterization of P2Y receptor subtypes functionally expressed on neonatal rat cardiac myofibroblasts. Br J Pharmacol 58:339–353
38. Thaning P, Bune LT, Hellsten Y, Pilegaard H, Saltin B, Rosenmeier JB (2010) Attenuated purinergic receptor function in patients with type 2 diabetes. Diabetes 59:182–189
39. Tsang S, Woo AY, Zhu W, Xiao RP (2010) Deregulation of RGS2 in cardiovascular diseases. Front Biosci (Schol Ed) 2:547–557
40. Vassort G (2001) Adenosine 5′-triphosphate: a P2-purinergic agonist in the myocardium. Physiol Rev 81:767–806
41. Von Kugelgen I (2006) Pharmacological profiles of cloned mammalian P2Y-receptor subtypes. Pharmacol Ther 110:415–432
42. Waldo GL, Harden TK (2004) Agonist binding and Gq-stimulating activities of the purified human $P2Y_1$ receptor. Mol Pharmacol 65:426–436
43. Wihlborg AK, Balogh J, Wang L, Borna C, Dou Y, Joshi BV, Lazarowski E, Jacobson KA, Arner A, Erlinge D (2006) Positive inotropic effects by uridine triphosphate (UTP) and uridine diphosphate (UDP) via $P2Y_2$ and $P2Y_6$ receptors on cardiomyocytes and release of UTP in man during myocardial infarction. Circ Res 98:970–976
44. Yasuda Y, Matsuura H, Ito M, Matsumoto T, Ding WG, Horie M (2005) Regulation of the muscarinic $K^+$ channel by extracellular ATP through membrane phosphatidylinositol 4,5-bisphosphate in guinea-pig atrial myocytes. Br J Pharmacol 145:156–165

*Original Article*

jraas

Journal of the Renin-Angiotensin-Aldosterone System
0(0) 1–7

DOI: 10.1177/1470320312474855
jra.sagepub.com
SAGE

# Irbesartan-mediated $AT_1$ receptor blockade attenuates hyposmotic-induced enhancement of $I_{Ks}$ current and prevents shortening of action potential duration in atrial myocytes

**Jie Wu[1,2,3], Wei-Guang Ding[2], Jin Zhao[1], Wei-Jin Zang[1], Hiroshi Matsuura[2] and Minoru Horie[3]**

## Abstract

*Introduction*: Stretch of the atrial membrane upregulates the slow component of delayed rectifier $K^+$ current ($I_{Ks}$). Blockade of angiotensin II subtype 1 receptors ($AT_1R$) attenuates this increase in $I_{Ks}$. The present study aimed to examine the effects of irbesartan, a selective $AT_1R$ blocker (ABR), on both the enhancement of $I_{Ks}$ and the shortening of action potential duration (APD) induced by stretching atrial myocytes for exploring the mechanisms underlying the prevention of atrial fibrillation (AF) by ABR.

*Methods*: Hyposmotic solution (Hypo-S) was used to stretch guinea pig atrial myocytes. $I_{Ks}$ and APD were recorded using the whole-cell patch-clamp technique.

*Results*: Irbesartan (1–50 μM) attenuated the Hypo-S-induced increase in $I_{Ks}$ and shortening of $APD_{90}$. Hypo-S increased the $I_{Ks}$ by 113.4%, whereas Hypo-S + 1 μM irbesartan and Hypo-S + 50 μM irbesartan increased the $I_{Ks}$ by only 74.5% and 70.3%, respectively. In addition, Hypo-S shortened the $APD_{90}$ by 19.0%, whereas Hypo-S + 1 μM irbesartan and Hypo-S + 50 μM irbesartan shortened the $APD_{90}$ by 12.1% and 12.0%, respectively.

*Conclusion*: The actions of irbesartan on electrical changes induced by stretching atrial myocytes are associated with blocking $AT_1R$. These actions may be beneficial for treating AF.

## Keywords

Angiotensin II type 1 receptor, irbesartan, atrial myocytes, $I_{Ks}$, action potential

## Introduction

Increasing evidence suggests that the renin–angiotensin system (RAS) is associated with the occurrence of atrial arrhythmias in experimental animals.[1–5] Recent clinical studies[6–11] have also suggested that blockade of the RAS with angiotensin-converting enzyme (ACE) inhibitors or angiotensin II (Ang II) type 1 receptor ($AT_1R$) blockers is effective for the treatment of atrial fibrillation (AF). However, mechanisms underlying the treatment are not fully understood, especially concerning actions of the drugs on electrical changes in AF.

The shortening of action potential duration (APD) and effective refractory period (ERP) are generally regarded as pivotal factors for the occurrence of reentry-based AF. During AF, impaired atrial contraction causes the atria to dilate or stretch[12,13] and induce the secretion of Ang II from cardiomyocytes.[14,15] Zankov et al. demonstrated that both exogenous Ang II and hyposmotic-induced membrane stretch potentiates the slow component of delayed rectifier $K^+$ current ($I_{Ks}$) in guinea pig myocytes by activating $AT_1R$, which results in a shortened atrial APD. These results suggest that the shortening of the atrial APD, associated with $I_{Ks}$ enhancement through the activation of $AT_1R$, plays an important role in facilitating the initiation/maintenance of AF.[16,17] Irbesartan, a selective $AT_1R$ blocker, was reported to

[1]Department of Pharmacology, Medical School of Xi'an Jiaotong University, PR China
[2]Department of Physiology, Shiga University of Medical Science, Japan
[3]Department of Cardiovascular and Respiratory Medicine, Shiga University of Medical Science, Japan

**Corresponding author:**
Minoru Horie, Department of Cardiovascular and Respiratory Medicine, Shiga University of Medical Science, Otsu, Shiga 520-2192, Japan.
Email: horie@belle.shiga-med.ac.jp

inhibit heterologously expressed *KCNQ1/KCNE1* (encoding $I_{Ks}$) channels,[18] which may contribute to its anti-AF mechanism. However, the effective concentrations of the drug for blocking *KCNQ1/KCNE1* channels are far greater than the clinical therapeutic levels achieved in blood.[19,20]

In the present study, we examined the effects of irbesartan on both the increase in $I_{Ks}$ and the shortening of APD induced by hyposmotic solution (Hypo-S) in guinea pig atrial myocytes. The results show that the actions of the drug at therapeutically relevant concentrations on electrical changes induced by the stretching of the atrial cell membrane are, at least partially, associated with blocking $AT_1R$ and therefore beneficial for AF prevention.

## Materials and methods

### Isolation of guinea pig atrial myocytes

The experimental procedures were conducted in accordance with the guidelines established by the Animal Care and Use Committee of Shiga University of Medical Science (Shiga, Japan). Single atrial myocytes were enzymatically dissociated from the hearts of non-pregnant adult female Hartley guinea pigs (weighing 250–350 g) using a retrograde Langendorff perfusion method as previously described.[16]

### Solutions and chemicals

Normal Tyrode solution (140 mM NaCl, 5.4 mM KCl, 1.8 mM $CaCl_2$, 0.5 mM $MgCl_2$, 0.33 mM $NaH_2PO_4$, 5.5 mM glucose, and 5.0 mM 4-(2-hydroxyethyl)-1-piperazineethanesulfonic acid (HEPES), pH adjusted to 7.4 with NaOH) was used as "isosmotic" extracellular solution (Iso-S, average osmolality: ~285 mOsm/kg). "Hyposmotic" extracellular solution (Hypo-S, average osmolality: ~212 mOsm/kg) was prepared by simply reducing the NaCl concentration to 100 mM in the normal Tyrode solution as previously described.[17] The pipette solution contained 70 mM potassium aspartate, 50 mM KCl, 10 mM $KH_2PO_4$, 1 mM $MgSO_4$, 3 mM $Na_2$-ATP (Sigma), 0.1 mM $Li_2$-GTP (Roche Diagnostics GmbH, Mannheim, Germany), 5 mM ethylene glycol tetraacetic acid (EGTA), and 5 mM HEPES, with the pH adjusted to 7.2 with KOH. Irbesartan (Dainippon Sumitomo Pharma Co., Ltd, Osaka, Japan) was dissolved in dimethyl sulfoxide (DMSO, Sigma) to yield 50 mM stock solution and diluted with Iso-S or Hypo-S to concentrations of 1 and 50 μM, respectively. The concentration of DMSO in the final solution (< 0.1%, *V/V*) slightly increased (< 3.8%) the osmolality of 50 μM irbesartan + Hypo-S (or Iso-S), but had no effect on cell swelling (see Supplementary Materials) or $I_{Ks}$.

### Electrophysiological recordings and data analysis

Single atrial myocytes were either current- or voltage-clamped using the standard whole-cell patch-clamp technique with an EPC-8 patch-clamp amplifier (HEKA Electronics, Lambrecht, Germany). Data were low-pass filtered at 5 kHz, acquired at 2 kHz through a LIH-1600 analogue-to-digital converter (HEKA), and stored on a hard drive using PATCHMASTER software (HEKA). Borosilicate glass electrodes had a tip resistance of 2.5–4.0 MΩ when filled with the pipette solution. All experiments were performed at 36 ± 1°C. $I_{Ks}$ was elicited by depolarizing voltage-clamp steps given from a holding potential of −50 mV to various test potentials, under conditions that the $Na^+$ current was inactivated by setting the holding potential to −50 mV. The L-type $Ca^{2+}$ channel current ($I_{Ca,L}$) and the rapid component of delayed rectifier $K^+$ current ($I_{Kr}$) were blocked by 0.4 μmol/l nisoldipine (Bayer AG, Wuppertal-Elberfeld, Germany) and 0.5 μmol/l dofetilide (Sigma Chemical Co., MO, USA) added to the extracellular solution, respectively.

Variations of $I_{Ks}$ amplitude and the time course of the $I_{Ks}$ were determined by measuring the amplitude of tail currents elicited on repolarization to a holding potential of −50 mV following two seconds (s) of depolarization to +30 mV every 10 s. Voltage-dependence of $I_{Ks}$ activation was evaluated by fitting the *I-V* relation of the tail currents to a Boltzmann equation as follows: $I_{K,tail} = 1/(1+\exp((V_h - V_m)/k))$, where $I_{K,tail}$ is the tail current amplitude, $V_h$ is the voltage at half-maximal activation, $V_m$ is the test potential, and $k$ is the slope factor. The deactivation kinetics of $I_{Ks}$ was determined by fitting a single exponential function to the tail current trace. Cell membrane capacitance ($C_m$) was calculated on the basis of the capacitive transients during 20 ms voltage-clamp steps (± 5 mV), using the equation $C_m = \tau_C I_0/\Delta V_m(1-I_{ss}/I_0)$, where $\tau_C$ is the time constant of the capacitive transient, $I_0$ is the initial peak current amplitude, $I_{ss}$ is the steady-state current value, and $\Delta V_m$ is the amplitude of the voltage step (5 mV).

Action potentials were evoked in current-clamp mode at a rate of 0.2 Hz by suprathreshold current pulses of 2 ms duration applied through the patch electrode. The APD was measured at 90% repolarization ($APD_{90}$).

All of the averaged data are presented as mean ± S.E.M. with the number of experiments shown in parentheses. Statistical comparisons were evaluated using Student's *t* test or one-way analysis of variance (ANOVA) with Newman-Keuls post-hoc test, as appropriate. A $p < 0.05$ was considered statistically significant.

## Results

### Irbesartan does not affect the baseline $I_{Ks}$ but attenuates the Hypo-S-induced $I_{Ks}$ enhancement

Based on the concentration-dependent effect of irbesartan on *KCNQ1/KCNE1* channels that was previously reported in a Chinese Hamster Ovary (CHO) expression system,[18] we chose to examine the effects of 1–50 μM irbesartan on $I_{Ks}$

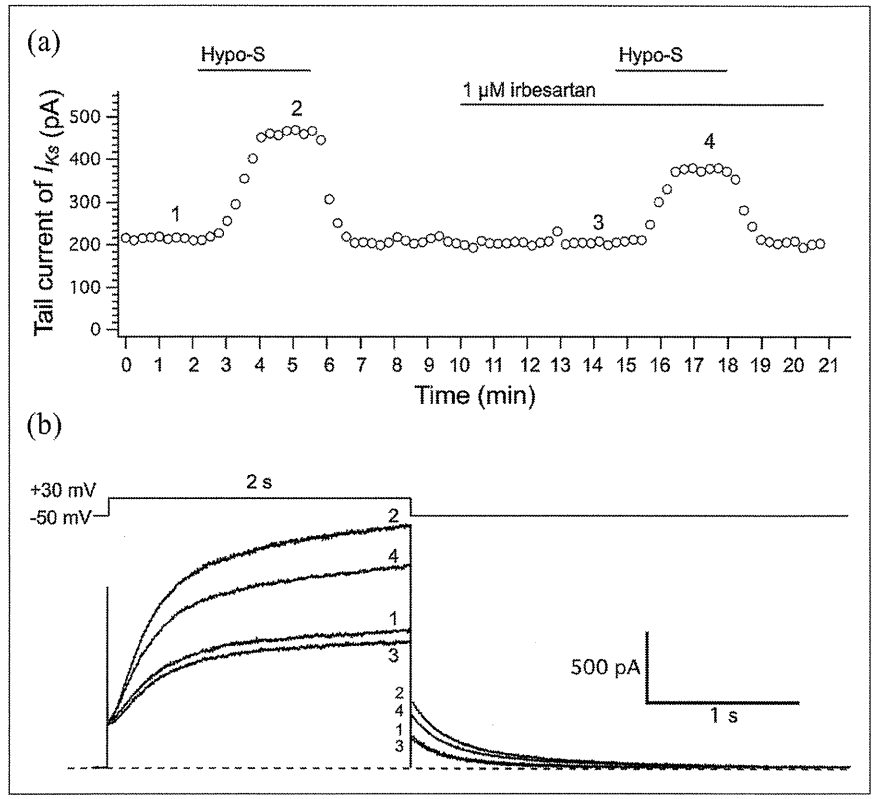


**Figure 1.** Irbesartan does not affect the baseline $I_{Ks}$ in guinea pig atrial myocytes.
(a) The representative time course of tail $I_{Ks}$ during the first and second (pretreatment with 1 μM irbesartan) exposures to Hypo-S. $I_{Ks}$ was repetitively (every 10 s) activated with 2 s depolarizing step to +30 mV from a holding potential of −50 mV, followed by a repolarization step to −50 mV. Current was determined by measuring and plotting the tail $I_{Ks}$ amplitude. (b) The superimposed $I_{Ks}$ traces recorded before (1) and during first exposure to Hypo-S (2). After washout with normal Tyrode and pretreatment with 1 μM irbesartan for five minutes (3), the same atrial myocyte was exposed to Hypo-S again (4). The dashed line indicates the zero current level. $I_{Ks}$: delayed rectifier $K^+$ current.

channels in guinea pig atrial myocytes, since 1–50 μM irbesartan are close to the therapeutic concentrations in blood[19,20] and almost the subthreshold for the inhibition of *KCNQ1/KCNE1* channels. Figure 1(a) depicts a representative time-course of atrial tail $I_{Ks}$ during the first and second exposures to Hypo-S that caused mechanical stretch of the cell membrane and induced enhancement of the $I_{Ks}$. Before the second exposure to Hypo-S, the myocyte was pretreated with irbesartan for five minutes. We found that 1–50 μM irbesartan did not affect the baseline $I_{Ks}$ of guinea pig atrial myocytes (current traces indicated by 1 and 3 in Figure 1(b)), which was quite similar to that in the CHO expression system.[18] As expected, Hypo-S induced increases in both steady-state and tail $I_{Ks}$ currents (current traces 2 and 4 in Figure 1(b)).

The myocyte swelling observed in Hypo-S reflects the effect of cell membrane stretching that usually occurs during the early stages of AF[12,21] and affects various ion transport mechanisms, including the $I_{Ks}$ enhancement in atrial myocytes.[17,22,23] Figures 2(a) and 2(b) show typical current traces elicited by depolarizing voltage-clamp steps given from a −50 mV holding potential to various test potentials in the absence (panel (a)) or presence of 1 μM irbesartan (panel (b)) while the cells were exposed to Hypo-S. Figure 2(c) summarizes the percentage increases of tail $I_{Ks}$ of cells in Hypo-S in the absence or presence of 1 and 50 μM irbesartan. The percentage increases in tail $I_{Ks}$ for the control cells and those in the presence of 1 and 50 μM irbesartan were 113.40 ± 9.96% ($n$ = 18), 74.52 ± 8.49% ($n$ = 10), and 70.25 ± 9.34% ($n$ = 16), respectively. Increases in tail $I_{Ks}$ in the presence of irbesartan were significantly lower ($p < 0.05$) than those in the control (Figure 2(c)). Figure 2(d) shows the current-voltage relationships for tail $I_{Ks}$ recorded during the superfusion with Iso-S (filled circles), Hypo-S (open circles), or Hypo-S + 1 μM irbesartan (open squares). The voltages for half-activation of tail $I_{Ks}$ ($V_h$) were obtained by fitting the data to the Boltzmann equation and were 9.06 ± 1.28 mV ($n$ = 22) in Iso-S, 2.08 ± 1.29 mV in Hypo-S ($n$ = 13; $p < 0.01$ vs. Iso-S), and 2.10 ± 1.70 mV in Hypo-S + 1 μM irbesartan ($n$ = 10; $p < 0.05$ vs. Iso-S), respectively. The Hypo-S caused a significant negative shift of $V_h$; however, irbesartan did not recover this negative shift in the activation gate. In addition, there were no significant differences in the parameters governing gating kinetics, irrespective of irbesartan treatment.

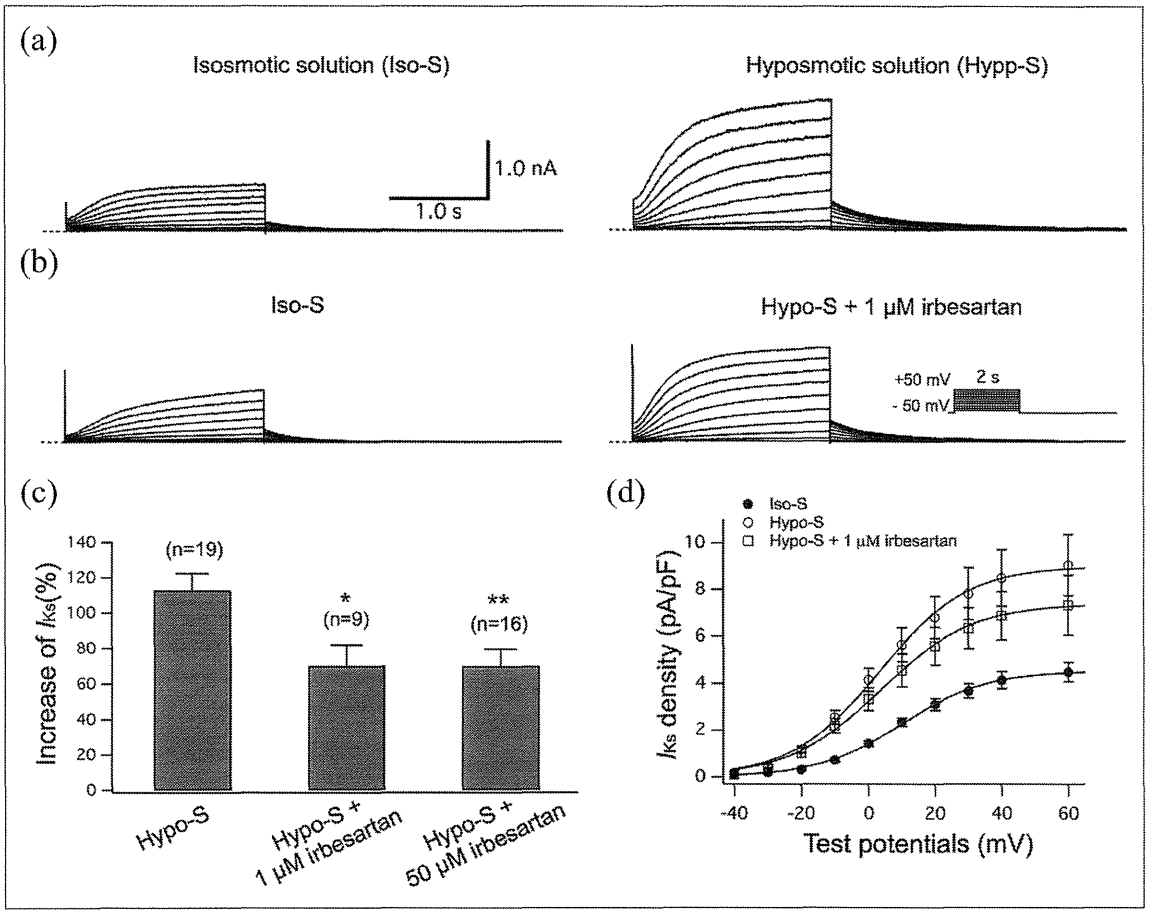


**Figure 2.** Irbesartan attenuates the Hypo-S-induced increase in $I_{Ks}$ in guinea pig atrial myocytes. The atrial myocytes were initially superfused with control Iso-S followed by Hypo-S in the absence (a) or presence of 1 μM irbesartan (b). $I_{Ks}$ was activated by depolarizing voltage-clamp steps given from a holding potential of −50 mV to potentials listed in the panel (b) inset. The dashed line indicates the zero current level. (c) The percentage increase in tail $I_{Ks}$ amplitudes induced by Hypo-S without and with irbesartan (1 μM and 50 μM) at +30 mV. (d) The *I-V* relations for tail $I_{Ks}$ amplitudes (expressed as current density) recorded during exposure to Iso-S (filled circles), Hypo-S (open circles), or Hypo-S + 1 μM irbesartan (open squares). Smooth curves through the data points denote the least-squares fit with the Boltzmann equation, yielding $V_h$ (see text). *$p < 0.05$ and **$p < 0.01$ vs. Hypo-S. $I_{Ks}$: delayed rectifier $K^+$ current.

Table 1 summarizes the effects of 1 μM irbesartan on the deactivation time course of tail $I_{Ks}$ at four different test potentials. The Hypo-S significantly ($p < 0.05$) slowed the deactivation time course of tail $I_{Ks}$ at voltages between −60 mV and −30 mV. There were, however, no significant differences in the increase of $\tau$ values (in parentheses) irrespective of irbesartan treatment, though there was a trend in the irbesartan-induced reduction of the Hypo-S effects on $I_{Ks}$ deactivation.

## *Irbesartan attenuates Hypo-S-induced shortening of the action potential*

Figure 3(a–c) shows the superimposed traces of guinea pig atrial action potentials in Iso-S and Hypo-S- (control, Figure 3(a)), Iso-S and Hypo-S + 1μM irbesartan- (Figure 3(b)), and Iso-S and Hypo-S + 50 μM (Figure 3(c)) irbesartan-treated myocytes, respectively. As the bar graphs summarize in Figure 3(d), Hypo-S shortened the $APD_{90}$ by 19.03 ± 1.36 ($n = 17$), whereas Hypo-S + 1 μM irbesartan shortened the $APD_{90}$ by only 12.05 ± 1.38 ($n = 9$; $p < 0.01$ vs. Hypo-S) and Hypo-S + 50 μM irbesartan shortened the $APD_{90}$ by 12.00 ± 1.46 ($n = 14$; $p < 0.01$ vs. Hypo-S). Together, these results suggest that 1–50 μM irbesartan significantly attenuated the Hypo-S-induced shortening of action potentials in atrial myocytes. In addition, no difference in depolarized resting membrane potentials caused by Hypo-S was observed between control cells and those in the presence of irbesartan (data not shown).

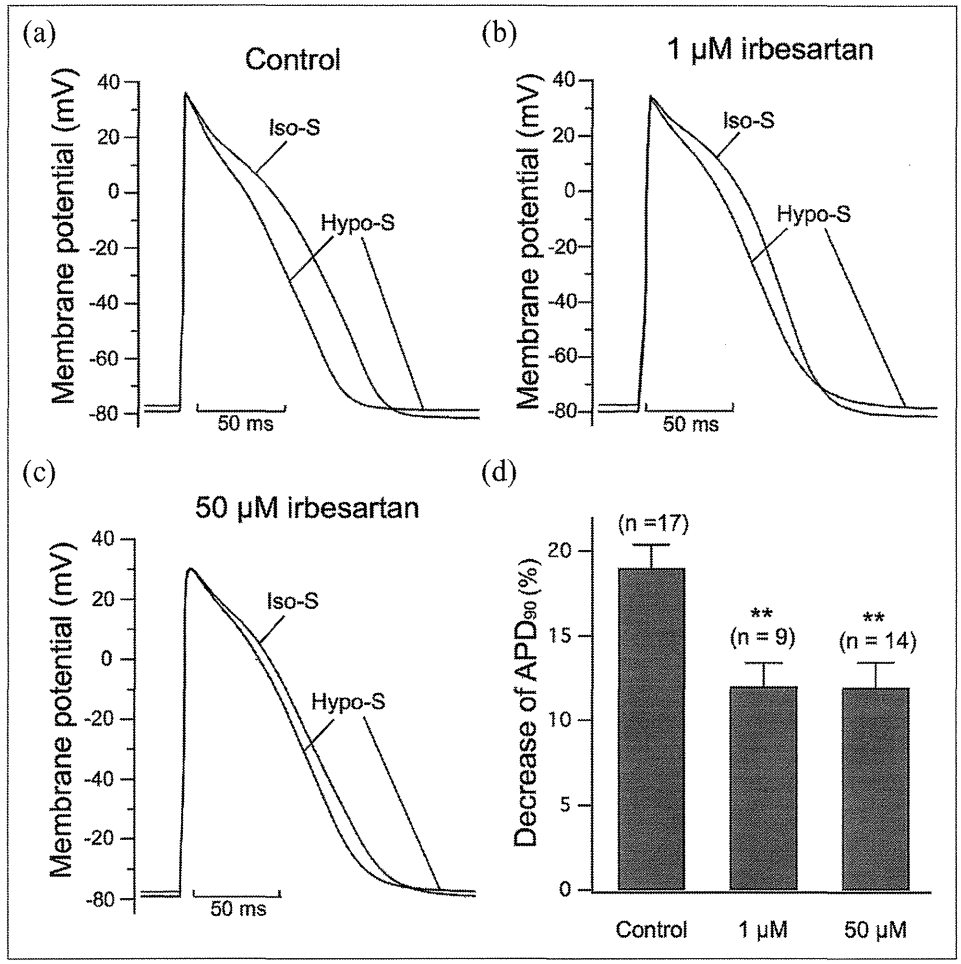


**Figure 3.** Irbesartan attenuates the Hypo-S-induced shortening of $APD_{90}$ in guinea pig atrial myocytes. Superimposed traces of action potentials in Iso-S followed by Hypo-S (a), Hypo-S + 1 μM irbesartan (b), or Hypo-S + 50 μM irbesartan (c), respectively. (d) The percentage decrease in $APD_{90}$ after exposure to Hypo-S without and then with irbesartan (1 μM and 50 μM). Although the effects of irbesartan on the shortening of $APD_{90}$ were significant, no statistical difference was observed in the resting membrane potentials. $^{**}p < 0.01$ vs. control.

**Table 1.** Effect of 1 μM irbesartan on deactivation time constants ($\tau$) of $I_{Ks}$ in isosmotic solution (Iso-S) and hyposmotic solution (Hypo-S) at four different test potentials.

| Parameters | Deactivation $\tau$ (ms) at different test potentials | | | | |
|---|---|---|---|---|---|
| | *N* | −60 mV | −50 mV | −40 mV | −30 mV |
| Iso-S | 27 | 194.9 ± 10.7 | 291.0 ± 18.5 | 426.2 ± 29.7 | 590.7 ± 43.9 |
| Hypo-S | 14 | 271.9 ± 21.2[b] | 398.2 ± 35.7[b] | 542.3 ± 52.2[a] | 678.2 ± 65.8 |
| (Δ%) | | (43.25 ± 5.15) | (41.57 ± 6.62) | (27.34 ± 4.09) | (16.17 ± 4.04) |
| Hypo-S + 1 μM irbesartan | 13 | 246.3 ± 23.6[a] | 357.8 ± 32.7 | 491.1 ± 46.0 | 622.3 ± 59.4 |
| (Δ%) | | (25.75 ± 7.67) | (23.99 ± 7.12) | (19.94 ± 6.67) | (7.84 ± 5.17) |

$I_{Ks}$: delayed rectifier $K^+$ current; N: number of cells; Δ%, percentage increase of $\tau$ values over Iso-S; data are expressed as the mean ± S.E.M.; $^a p < 0.05$ and $^b p < 0.01$ vs. Iso-S.

## Discussion

Cellular electrophysiological studies have indicated that the most important impact of AF on ion channels is the marked reduction in inward $I_{Ca,L}$ currents,[12] which leads to atrial contractile dysfunction and induces increased membrane stretching of outward $I_{Ks}$ currents.[17,21,22,24] Changes in both $I_{Ca,L}$ and $I_{Ks}$ contribute to the atrial APD shortening

and the loss of its physiological rate adaptation, which promotes atrial electrical and structural remodeling and creates a substrate for persistent AF.[12,23]

In the present study, we found that irbesartan attenuated the stretch-induced enhancement of $I_{Ks}$, suggesting that the drug possesses the ability to improve the pathophysiological conditions precipitating AF. This hypothesis is supported by the recent identification of *KCNQ1* (encoding the $\alpha$-subunit of the $I_{Ks}$ channel) S140G and R14C mutations in familial AF cases, in which both "gain-of-function" mutations cause an enhancement of $I_{Ks}$.[25,26] In addition, atrial membrane stretching results in an increase of $I_{Ks}$-mediated shortening of the atrial APD, which may facilitate the maintenance of AF.[17,27,28] Irbesartan can rescue shortening of the APD that is induced by cell membrane stretching. Thus, the inhibition of extreme APD shortening as a result of atrial membrane stretching is involved in the mechanism underlying irbesartan-mediated AF prevention.

Evidence suggests that the RAS plays a pivotal role in the occurrence and maintenance of AF. Atrial membrane stretching during AF not only activates $AT_1R$,[29,30] but also induces the secretion of Ang II from cardiomyocytes.[14,15] Madrid and colleagues[31] reported that irbesartan in combination with amiodarone was more effective at preventing the recurrence of AF than amiodarone alone. Several recent clinical reports[6–10] and animal experiments[2,32] have also confirmed the effect of $AT_1R$ blockers on AF. In the present study, therapeutically relevant concentrations of irbesartan attenuated the stretch-induced increase, but not baseline, levels of atrial $I_{Ks}$, suggesting that the action of the drug on electrical changes is associated with blocking $AT_1R$. This result is consistent with a previous study[33] that found that irbesartan prevented the arrhythmogenic effect of Ang II by blocking $AT_1R$ in human atrial myocardium. Zankov et al. reported that the selective $AT_1R$ blockers valsartan and candesartan attenuate Ang II- and stretch-induced enhancement of $I_{Ks}$ and shortening of APD, respectively, by activating $AT_1R$ in guinea pig atrial myocytes.[16,17] Based on these previous findings together with the observations of irbesartan in this study, we conclude that the actions of ARBs on electrical changes associated with the dilation or stretch of the atria are involved in the $AT_1R$ blockade and are beneficial for the prevention of acute electrical remodeling during AF.

In the present study, we also found that Hypo-S depolarized resting membrane potentials in guinea pig myocytes. Since the inward rectifier current $I_{K1}$ is responsible for maintaining the resting membrane potential,[23] and irbesartan did not affect the depolarization of the resting membrane potential caused by atrial membrane stretching, we postulate that $I_{K1}$ is not the therapeutic target of $AT_1R$ blockers during AF.[34] This lack of effect on the resting membrane potential was also observed with candesartan in a previous study.[17]

## Conclusions

Irbesartan-mediated $AT_1R$ blockade attenuates the electrical changes induced by stretching atrial myocytes. This is likely why AF patients derive a pronounced benefit with ABRs such as irbesartan.

### Acknowledgements

We thank Dainipon Sumitomo Pharma Co., Ltd (Osaka, Japan) and Sanofi-Aventis (France) for kindly providing us with irbesartan as a reagent.

### Conflict of interest

None declared.

### Funding

This work was supported, in part, by a Grant-in-Aid for Scientific Research from the Ministry of Education, Culture, Sports, Science and Technology (to MH); National Natural Science Foundation of China (#81273501 to JW and WGD, and #30930105 to WJZ); Major International (Regional) Joint Research Project of National Natural Science Foundation of China (#81120108002 to WJZ); Uehara Memorial Foundation; and the Ministry of Health, Labor and Welfare of Japan for Clinical Research on Measures for Intractable Diseases (to MH).

### References

1. Harada K, Komuro I, Hayashi D, et al. Angiotensin II type 1a receptor is involved in the occurrence of reperfusion arrhythmias. *Circulation* 1998; 97: 315–317
2. Kumagai K, Nakashima H, Urata H, et al. Effects of angiotensin II type I receptor antagonist on electrical and structural remodeling in atrial fibrillation. *J Am Coll Cardiol* 2003; 41: 2197–2204.
3. Galinier M, Pathak A and Roncalli J. Angiotensin receptor blockers and cardiac rhythm disorders. *Arch Mal Coeur Vaiss* 2006; 99: 745–747.
4. Ehrlich JR and Nattel S. Novel approaches for pharmacological management of atrial fibrillation. *Drugs* 2009; 69: 757–774.
5. Ko WC, Hong CY, Hou SM, et al. Elevated expression of connective tissue growth factor in human atrial fibrillation and angiotensin II-treated cardiomyocytes. *Circ J* 2011; 75: 1592–1600.
6. Madrid AH, Peng J, Zamora J, et al. The role of angiotensin receptor blockers and/or angiotensin converting enzyme inhibitors in the prevention of atrial fibrillation in patients with cardiovascular diseases: Meta-analysis of randomized controlled clinical trials. *Pacing Clin Electrophysiol* 2004; 27: 1405–1410.
7. Wachtell K, Lehto M, Gerdts E, et al. Angiotensin II receptor blockade reduces new-onset atrial fibrillation and subsequent stroke compared to atenolol: The Losartan Intervention For End Point Reduction in Hypertension (LIFE) study. *J Am Coll Cardiol* 2005; 45: 712–719.

8. Healey JS, Baranchuk A, Crystal E, et al. Prevention of atrial fibrillation with angiotensin-converting enzyme inhibitors and angiotensin receptor blockers: A meta-analysis. *J Am Coll Cardiol* 2005; 45: 1832–1839.
9. Novo G, Guttilla D, Fazio G, et al. The role of the renin-angiotensin system in atrial fibrillation and the therapeutic effects of ACE-Is and ARBS. *Br J Clin Pharmacol* 2008; 66: 345–351.
10. Schneider MP, Hua TA, Bohm M, et al. Prevention of atrial fibrillation by rennin-angiotensin system inhibition a meta-analysis. *J Am Coll Cardiol* 2010; 55: 2299–2307.
11. L'Allier PL, Ducharme A, Keller PF, et al. Angiotensin-converting enzyme inhibition in hypertensive patients is associated with a reduction in the occurrence of atrial fibrillation. *J Am Coll Cardiol* 2004; 44: 159–164.
12. Allessie M, Ausma J and Schotten U. Electrical, contractile and structural remodeling during atrial fibrillation. *Cardiovasc Res* 2002; 54: 230–246.
13. Nattel S. New ideas about atrial fibrillation 50 years on. *Nature* 2002; 415: 219–226.
14. Sadoshima J, Xu Y, Slayter HS, et al. Autocrine release of angiotensin II mediates stretch-induced hypertrophy of cardiac myocytes in vitro. *Cell* 1993; 75: 977–984.
15. Gassanov N, Brandt MC, Michels G, et al. Angiotensin II-induced changes of calcium sparks and ionic currents in human atrial myocytes: Potential role for early remodeling in atrial fibrillation. *Cell Calcium* 2006; 39: 175–186.
16. Zankov DP, Omatsu-Kanbe M, Isono T, et al. Angiotensin II potentiates $I_{Ks}$ potassium current via $AT_1$ receptors in guinea-pig atrial myocytes. *Circulation* 2006; 113: 1278–1286.
17. Zankov DP, Toyoda F, Omatsu-Kanbe M, et al. Angiotensin II type 1 receptor mediates partially hyposmotic-induced increase of $I_{Ks}$ current in guinea pig atrium. *Pflugers Arch* 2009; 458: 837–849.
18. Moreno I, Caballero R, Gonzalez T, et al. Effects of irbesartan on cloned potassium channels involved in human cardiac repolarization. *J Pharmacol Exp Ther* 2003; 304: 862–873.
19. Markham A, Spencer C and Jarvis B. Irbesartan: An update review of its use in cardiovascular disorders. *Drugs* 2000; 59: 1187–1206.
20. Tutunji LF, Tutunji MF, Alzoubi MI, et al. Simultaneous determination of irbesartan and hydrochlorothiazide in human plasma using HPLC coupled with tandem mass spectrometry: Application to bioequivalence studies. *J Pharm Biomed Anal* 2010; 51: 985–990.
21. Sasaki N, Mitsuiye T, Wang Z, et al. Increase of the delayed rectifier $K^+$ and $Na^+$–$K^+$ pump currents by hypotonic solutions in guinea pig cardiac myocytes. *Circ Res* 1994; 75: 887–895.
22. Kocic I. Modulators of ion channels activated by hypotonic swelling in cardiomyocytes: New perspectives for pharmacological treatment of life-threatening arrhythmias. *Curr Med Chem Cardiovasc Hematol Agents* 2005; 3: 333–339.
23. Schotten U, Verheule S, Kirchhof P, et al. Pathophysiological mechanisms of atrial fibrillation: A translational appraisal. *Physiol Rev* 2011; 91: 265–325.
24. Rees SA, Vandenberg JI, Wright AR, et al. T. Cell swelling has differential effects on the rapid and slow components of delayed rectified potassium current in guinea pig cardiac myocytes. *J Gen Physiol* 1995; 106: 1151–1170.
25. Otway R, Vandenberg JI, Guo G, et al. Stretch-sensitive KCNQ1 mutation: A link between genetic and environmental factors in the pathogenesis of atrial fibrillation? *J Am Coll Cardiol* 2007; 49: 578–586.
26. Chen YH, Xu SJ, Bendahhou S, et al. KCNQ1 gain-of-function mutation in familial atrial fibrillation. *Science* 2003; 299: 251–254.
27. Vandenberg JI, Bett GC and Powell T. Contribution of a swelling-activated chloride current to changes in the cardiac action potential. *Am J Physiol Cell Physiol* 1997; 42: C541–C547.
28. Kocic I, Hirano Y and Hiraoka M. Ionic basis for membrane potential changes induced by hypoosmotic stress in guinea-pig ventricular myocytes. *Cardiovasc Res* 2001; 51: 59–70.
29. Zou Y, Akazawa H, Qin Y, et al. Mechanical stress activates angiotensin II type 1 receptor without the involvement of angiotensin II. *Nat Cell Biol* 2004; 6: 499–506.
30. Yasuda N, Miura S, Akazawa H, et al. Conformational switch of angiotensin II type 1 receptor underlying mechanical stress-induced activation. *EMBO Rep* 2008; 9: 179–186.
31. Madrid AH, Bueno MG, Rebollo JM, et al. Use of irbesartan to maintain sinus rhythm in patients with long-lasting persistent atrial fibrillation: A prospective and randomized study. *Circulation* 2002; 106: 331–336.
32. Nakashima H, Kumagai K and Urata H. Angiotensin II antagonist prevents electrical remodeling in atrial fibrillation. *Circulation* 2000; 101: 2612–2617.
33. Von Lewinski D, Kockskamper J, Rubertus SU, et al. Direct pro-arrhythmogenic effects of angiotensin II can be suppressed by $AT_1$ receptor blockade in human atrial myocardium. *Eur J Heart Fail* 2008; 10: 1172–1176.
34. Ehrlich JR. Inward rectifier potassium currents as a target for atrial fibrillation therapy. *J Cardiovasc Pharmacol* 2008; 52: 129–135.

# Identification of high-risk syncope related to ventricular fibrillation in patients with Brugada syndrome

Yutaka Take, MD,* Hiroshi Morita, MD,*† Norihisa Toh, MD,* Nobuhiro Nishii, MD,* Satoshi Nagase, MD,* Kazufumi Nakamura, MD,* Kengo F. Kusano, MD,* Tohru Ohe, MD, FHRS,‡ Hiroshi Ito, MD*

*From the *Department of Cardiovascular Medicine Okayama University Graduate School of Medicine, Dentistry and Pharmaceutical Sciences, †Department of Cardiovascular Therapeutics, Okayama University Graduate School of Medicine, Dentistry and Pharmaceutical Sciences, Okayama, Japan; ‡Department of Cardiovascular Medicine, Sakakibara Heart Institute of Okayama, Okayama, Japan.*

**BACKGROUND** Syncope in patients with Brugada syndrome is usually associated with ventricular tachyarrhythmia, but some episodes of syncope can be related to autonomic disorders.

**OBJECTIVE** The purpose of this study was to investigate the characteristics of syncope to differentiate high-risk syncope episodes from low-risk events in patients with Brugada syndrome.

**METHODS** We studied 84 patients with type 1 electrocardiogram and syncope. Patients were divided into 2 groups: patients with prodrome (prodromal group; n = 41) and patients without prodrome (nonprodromal group; n = 43).

**RESULTS** Ventricular fibrillation (VF) was documented at index event in 19 patients: 4 patients (21%) with documented VF experienced a prodrome prior to the onset of VF, whereas 15 patients (79%) did not have symptoms prior to documented VF ($P < .01$). Twenty-seven patients in the prodromal group and 7 patients in the nonprodromal group were considered to have syncope related to autonomic dysfunction. Syncope in other patients was defined as unexplained syncope. During the follow-up period (48 ± 48 months), recurrent syncope due to VF occurred in 13 patients among patients with only unexplained syncope and was more frequent in the nonprodromal group (n = 10) than in the prodromal group (n = 3; $P = .044$). In multivariate analysis, blurred vision (hazard ratio [HR] 0.20) and abnormal respiration (HR 2.18) and fragmented QRS (HR 2.39) were independently associated with the occurrence of VF.

**CONCLUSION** Syncope with prodrome, especially blurred vision, suggests a benign etiology of syncope in patients with Brugada syndrome.

**KEYWORDS** Brugada syndrome; Neurally mediated syncope; Prodrome; Syncope; Ventricular fibrillation

**ABBREVIATIONS** **BS** = Brugada syndrome; **ECG** = electrocardiogram; **f-QRS** = fragmented QRS; **HUT** = head-up tilt; **ICD** = implantable cardioverter-defibrillator; **NMS** = neurally mediated syncope; **OH** = orthostatic hypotension; **VF** = ventricular fibrillation



## Introduction

Syncopal episodes in patients with Brugada syndrome (BS) are usually associated with the occurrence of ventricular tachyarrhythmias. Spontaneous type 1 electrocardiogram (ECG) and episodes of syncope are predictors of sudden cardiac arrest in patients with BS.[1–4] However, patients with BS often have autonomic nerve disorders,[5,6] and some of their episodes of syncope can result from low-risk events (such as neurally mediated syncope [NMS] or orthostatic hypotension [OH]). In the general population, NMS has been shown to be one of the major causes of syncope.[7] Although syncopal episodes associated with autonomic disorders usually have prodromal symptoms and occur in specific situations, differentiation of low-risk episodes from high-risk syncopal episodes due to ventricular tachyarrhythmias is often difficult in patients with BS. Moreover, vagal nerve activation causes NMS as well as exaggeration of ST-segment elevation and induces ventricular fibrillation (VF) in patients with BS.[8] It is possible that vagal nerve activation initiates NMS-like symptoms and subsequently induces VF. Determination of the etiology of syncope episodes is important to identify patients with BS who are at risk of sudden cardiac arrest and who require an implantable cardioverter-defibrillator (ICD). When vagal nerve activation induces VF, prodrome accompanied by vagal nerve activation can appear immediately before the episodes. In the present study, we investigated the characteristics of syncope and determined high-risk syncope associated with ventricular arrhythmias to differentiate high-risk syncope episodes from low-risk events. We also determined whether

**Address reprint requests and correspondence:** Dr Hiroshi Morita, MD, Department of Cardiovascular Medicine/Cardiovascular Therapeutics, Okayama University Graduate School of Medicine, Dentistry and Pharmaceutical Sciences, 2-5-1 Shikata-Cho, Okayama City, Okayama 700-8558, Japan. E-mail address: hmorita@cc.okayama-u.ac.jp.

1547-5271/$ -see front matter © 2012 Heart Rhythm Society. All rights reserved. doi:10.1016/j.hrthm.2011.11.045

patients have any prodrome before VF in association with vagal nerve activation.

## Methods

We first enrolled 92 patients with a history of syncope and faintness who had BS-like ECGs. We excluded 7 patients because of inability to confirm type 1 ECG by the consensus report of BS[2] spontaneously or after a drug-provocation test. We also excluded 1 patient with a history of VF due to ischemic heart disease who had undergone coronary-artery bypass surgery for triple vessel disease. Therefore, this study group comprised 82 males and 2 females with BS (mean age 47 ± 12 years). All patients had episodes of syncope (76 patients) or faintness (8 patients) and had type 1 ECG (61 spontaneous and 23 pilsicainide-induced). We divided the patients into 2 groups according to syncope episodes associated with the existence of prodrome: patients with prodromal symptoms or specific situations (prodromal group; n = 41) and patients without any prodromal symptoms or specific situations (nonprodromal group; n = 43). We defined prodromal symptoms as blurred vision, diaphoresis, palpitations, chest discomfort, and symptoms associated with urination.

No patients were from the same family. Echocardiography and chest radiography were performed in all patients, and no abnormalities were found. We interviewed all patients at the time of history to obtain information on situations and characteristics of syncope. The follow-up duration was defined as the time between the first event and the final visit date. The mean follow-up duration of all patients was 48 ± 48 months. Syncope was classified on the basis of the European Society of Cardiology guidelines for the diagnosis and management of syncope (version 2009).[9] NMS was diagnosed by the combination of results of a head-up tilt (HUT) test[9] and situations and symptoms of syncopal episodes. Documentation of VF was defined as cardiopulmonary arrest at the hospital or in the ambulance. Detection of VF was defined as records of continuous ECG monitoring, automated external defibrillator, and ICD.

The HUT test[9] was performed in 35 patients (25 patients in the prodromal group and 10 patients in the nonprodromal group). The test was performed in the late afternoon in a fasting state. An intravenous line was inserted before the HUT test. Each patient lay on the tilt table in the supine position for 10 minutes at first. Then the tilt table was kept at an angle of 75° for 20 minutes. When the passive control test result was negative, the patient was returned to the supine position. Thereafter, low-dose isoproterenol infusion (≈0.01−0.03 μg/kg/min) was started to increase the heart rate. After an increase of more than 20% over baseline in the heart rate had been achieved, the tilt table was again kept at an angle of 75° for 25 minutes. A positive HUT test was defined as appearance of syncope or presyncope associated with reflex hypotension or bradycardia. The HUT response was classified as cardioinhibitory, vasodepressor, or mixed type on the basis of the predominancy of cardioinhibitory or vasodepressor reflex.

Standard 12-lead ECGs (0−150-Hz filter) and additional $V_1$-$V_3$ at the 3rd intercostal space were recorded simultaneously. We evaluated the RR, PQ, and QRS intervals in lead II as well as the QT interval, ST level at J point, and existence of fragmented QRS (f-QRS) in leads $V_1$-$V_3$ of the 12-lead ECG at the patients' first visit. We previously reported that type 0 ECG was defined as coved ST-segment elevation ≥ 2 mm with an absent or shallow negative T wave (depth ≤ 1 mm)[10] (Figure 1).

The presence of late potential was evaluated with a signal-averaged ECG (ART 1200EPX, noise level < 0.3 μV, and high-pass filtering of 40 Hz with a bidirectional 4-pole Butterworth). The filtered QRS duration, root-mean-square voltage of the terminal 40 ms in the filtered QRS complex, and duration of low-amplitude signals <40 μV in the terminal filtered QRS complex were measured by the signal-averaged ECG. Late potentials (LPs) were considered to be positive when the following 2 criteria were met: root-mean-square voltage of the terminal 40 ms in the filtered QRS complex < 20 μV and duration of low-amplitude signals <40 μV in the terminal filtered QRS complex > 38 ms.[11]

All the patients who underwent an electrophysiological study had received an explanation of the risks involved and had provided written informed consent. The electrophysiological study was performed in 72 patients. All those patients underwent coronary angiography, and none of the patients had significant coronary artery stenosis. Induction of ventricular arrhythmia was attempted by programmed electrical stimulation from the right ventricular apex, right ventricular outflow, and left ventricle, with a maximum of 3 extrastimuli at 2 cycles.[12,13] The criterion for the induction of ventricular arrhythmia was the induction of sustained polymorphic ventricular tachycardia or VF with double or less extrastimuli.

The genetic analysis of *SCN5A* was performed in 46 patients as previously described[14] in compliance with guidelines for human genome studies of the ethics committee of Okayama University.

## Statistics

Continuous data were expressed as means ± standard deviation. Comparisons among means were performed with a 2-way analysis of variance coupled with Scheffe's test. A comparison of 2 groups was made with the Student *t* test for unpaired data (patients' data), as appropriate. Categorical data and percentage frequencies were analyzed by using a nonparametric test (Man-Whitney *U* test). The Fisher exact test was conducted for a comparison of proportions between the groups. Survival and event rates were determined by using the Kaplan-Meier method and compared between the groups with a 2-sample log-rank test. We compared clinical parameters and prognosis between the prodromal and nonprodromal groups, and then we used Cox proportional hazards model to detect risk factors of VF. To examine prognostic values from predictors of VF and determine cutoff values, an analysis of receiver-operating characteristic

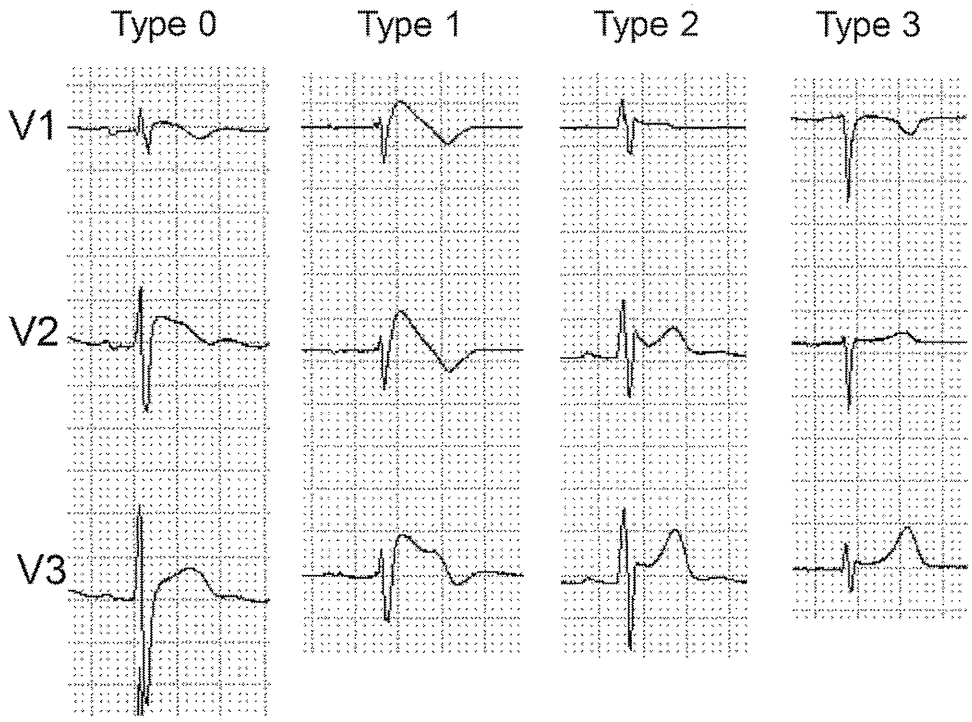


**Figure 1** Types of ECGs in patients with Brugada syndrome. **A:** Type 0 is defined as ECG with coved ST-segment elevation ≥ 2 mm and a shallow negative T wave (≤1 mm) or having no negative T wave. **B–D:** Type 1–3 ECGs are defined according to the consensus reports of Brugada syndrome. ECG = electrocardiogram.

curves was done. Significance was defined as $P < .05$. JMP version 7.0 (SAS Institute, Inc, Cary, NC) was used for data analysis.

## Results

### Clinical characteristics and ECG parameters in the prodromal and nonprodromal groups

There was no difference in the baseline characteristics between the prodromal group and the nonprodromal group (Table 1). VF during the follow-up period in patients without VF documentation at their index hospitalization was more frequent in the nonprodromal group than in the prodromal group (Figure 2A). The percentage of patients in the nonprodromal group who received ICD implantation was higher than that in the prodromal group (Table 1). There were no differences in the inducibility of VF by programmed electrical stimulations, incidence of family history of sudden death, and frequency of *SCN5A* mutation between the prodromal group and the nonprodromal group. In ECG parameters, the nonprodromal group had a longer PQ interval in lead II and a longer QT interval in lead $V_1$ than those in the prodromal group. There were no differences in the indices of ECG types and f-QRS between the 2 groups. The filtered QRS interval in the signal-averaged ECG was longer in the nonprodromal group than in the prodromal group.

### Features of syncope

Table 2 shows clinical characteristics of syncope. There were no differences in incidences of syncope and faintness between the 2 groups. Patients in the prodromal group experienced prodrome immediately before episodes of syncope or faintness: blurred vision was the most common prodrome, and about one-third of the patients experienced syncope in association with urination. Abnormal respiration was frequently observed in the nonprodromal group. There were no differences in the frequencies of convulsion, incontinence, and injury between the 2 groups.

Syncope often occurred in the supine position during sleep in patients in the nonprodromal group. Patients in the prodromal group often experienced syncope while they were standing, and this resulted in falling down after the episode. There were no differences in other syncope between the 2 groups. A positive HUT test result was observed more frequently in the prodromal group (54%) than in the nonprodromal group (10%, $P = .012$).

Table 3 shows the clinical characteristics of syncope in patients without VF detection at index hospitalization. When subjects were limited to patients who did not have VF at index hospitalization, blurred vision was the most common prodrome in the prodromal group. The clinical features of these patients' subgroups were similar to the data including patients who had VF at index hospitalization (Tables 2 and 3).

### Causes of syncope

At the time of index hospitalization, VF was documented in 19 patients (4 in the prodromal group and 15 in the nonprodromal group) and was not documented in 65 patients (37 in the prodromal group and 28 in the nonprodromal group) (Table 2 and Figure 2A). One patient in the nonpro-

**Table 1** Clinical and ECG parameters in patients with and without prodromal symptoms

| Variables | Prodromal group | Nonprodromal group | *P* |
|---|---|---|---|
| Number of patients | 41 | 43 | |
| Clinical parameters | | | |
| Age (y) | 46 ± 11 | 48 ± 13 | NS |
| Female gender | 1 (2%) | 1 (2%) | NS |
| Family history | 11 (27%) | 10 (23%) | NS |
| *SCN5A* mutation | 7/18 (39%) | 13/28 (46%) | NS |
| Inducible VF/VT at PES | 19/35 (54%) | 19/37 (52%) | NS |
| Follow-up period (m) | 44 ± 42 | 52 ± 52 | NS |
| ICD implantation | 14 (34%) | 31 (72%) | .00036 |
| ECG parameters | | | |
| ECG type | | | |
| Type 1 | 28 (68%) | 33 (77%) | NS |
| Type 0 | 16 (39%) | 16 (39%) | NS |
| RR II (ms) | 963 ± 164 | 991 ± 183 | NS |
| PQ II (ms) | 170 ± 21 | 182 ± 27 | .029 |
| QRS II (ms) | 111 ± 18 | 112 ± 20 | NS |
| QT | | | |
| $V_1$ (ms) | 385 ± 33 | 403 ± 39 | .027 |
| $V_2$ (ms) | 400 ± 39 | 413 ± 38 | NS |
| $V_3$ (ms) | 393 ± 33 | 406 ± 38 | NS |
| ST level | | | |
| $V_1$ (mV) | 0.19 ± 0.10 | 0.26 ± 0.26 | NS |
| $V_2$ (mV) | 0.33 ± 0.16 | 0.41 ± 0.32 | NS |
| $V_3$ (mV) | 0.21 ± 0.09 | 0.25 ± 0.18 | NS |
| Fragmented QRS | | | |
| Number of spikes | | | |
| $V_1$ | 2.7 ± 0.8 | 2.8 ± 1.0 | NS |
| $V_2$ | 2.5 ± 1.3 | 3.0 ± 1.2 | NS |
| $V_3$ | 2.0 ± 1.1 | 2.3 ± 1.0 | NS |
| Total spikes | 7.2 ± 2.6 | 8.1 ± 2.7 | NS |
| Existence of f-QRS | 14 (34%) | 23 (50%) | NS |
| Signal averaged ECG | | | |
| Filtered QRS (ms) | 119 ± 16 | 130 ± 21 | .012 |
| LAS40 (ms) | 45 ± 14 | 49 ± 15 | NS |
| RMS40 ($\mu$V) | 15 ± 9 | 12 ± 9 | NS |
| Late potential positive | 27 (66%) | 34 (79%) | NS |

Values represent n (%) and mean ± standard deviation.

ECG = electrocardiogram; f-QRS = fragmented QRS; ICD = implantable cardioverter-defribillator; LAS40 = duration of low-amplitude signals <40 $\mu$V in the terminal filtered QRS complex; NS = nonsignificant; PES = programmed electrical stimulation; RMS40 = root-mean-square voltage of the terminal 40 ms in the filtered QRS complex; VF = ventricular fibrillation; VT = ventricular tachijcardia.

dromal group who had syncope episodes coincident with bradyarrhythmia was diagnosed as having sick sinus syndrome. Among 64 patients without documented VF at their index hospitalization, we considered causes of syncope to be NMS in 21 patients (all in the prodromal group) and OH in 13 patients (6 in the prodromal group and 7 in the nonprodromal group) on the basis of results of HUT tests and situations of the episodes, but we could not determine the cause of syncope in 30 patients (unexplained syncope: 10 in the prodromal group and 20 in the nonprodromal group). VF was documented at the time of recurrent syncope in 13 patients with unexplained syncope and was more frequent in the nonprodromal group (n = 10) than in the prodromal group (n = 3; $P$ = .044) during the follow-up period (Figures 2A and 2B). One patient in the nonprodromal group was diagnosed with epilepsy during follow-up. None of the patients diagnosed with NMS or OH experienced VF during follow-up.

## Predictors of VF

Table 4 shows results of univariate analysis for the prediction of VF in clinical and ECG parameters between patients with VF and patients without VF. In this table, documentation of VF includes both VF at index hospitalization and VF during the follow-up period. Clinical parameters were not different between patients with documented VF (VF group) and patients without documented VF (non-VF group). In ECG parameters, appearance of spontaneous type 1 or type 0 ECG, prolonged QT interval in leads $V_1$ and $V_2$, and existence of f-QRS were associated with the occurrence of VF (Table 4). Although prodrome was usually related to non-VF episodes, about 20% of the patients in the VF group experienced prodrome before the onset of VF (Table 5): prodromal symptoms before VF were blurred vision (rare), palpitations, and chest discomfort. VF often occurred at rest in the supine position and was accompanied by convulsion and abnormal respiration during the episode. Non-VF episodes usually occurred with prodrome (especially blurred vision and diaphoresis) while patients were standing or urinating.

Figures 2B and 2C show results of the Kaplan-Meier analysis of the new occurrence of VF in patients without documented VF at their index hospitalization. Absence of prodrome (especially blurred vision, relation to urination, and diaphoresis) was associated with the subsequent occurrence of VF episodes during the follow-up period (Figure 2C).

Table 6 shows results of univariate analysis for the prediction of VF in patients with BS. Prodromal symptoms (especially blurred vision) and syncope while standing were low-risk symptoms for the occurrence of VF, and syncope without prodrome was a predictor of VF occurrence during follow-up. Abnormal respiration and convulsion during the episode were related to the occurrence of VF. Appearance of type 0 or type 1 ECG and existence of late potential or f-QRS were also predictors of VF.

Multivariate analysis that included the variables listed in Table 6 indicated that syncope with blurred vision was a low-risk symptom for the occurrence of VF and that abnormal respiration and f-QRS were independent risk factors for the occurrence of VF. Receiver-operating characteristic curves for patients with VF showed that absence of blurred vision had high sensitivity (93.8%) but low specificity (50.0%), abnormal respiration had low sensitivity (43.8%) but high specificity (92.3%), and f-QRS had intermediate sensitivity (71.9%) and specificity (73.1%). Figure 2D shows that the receiver-operating characteristic curve was graphed by the combination of fQRS, abnormal respiration, and absence of blurred vision. This combination had an excellent accuracy of diagnosis for patients with VF (sensitivity of 84.4% and specificity of 82.7%).

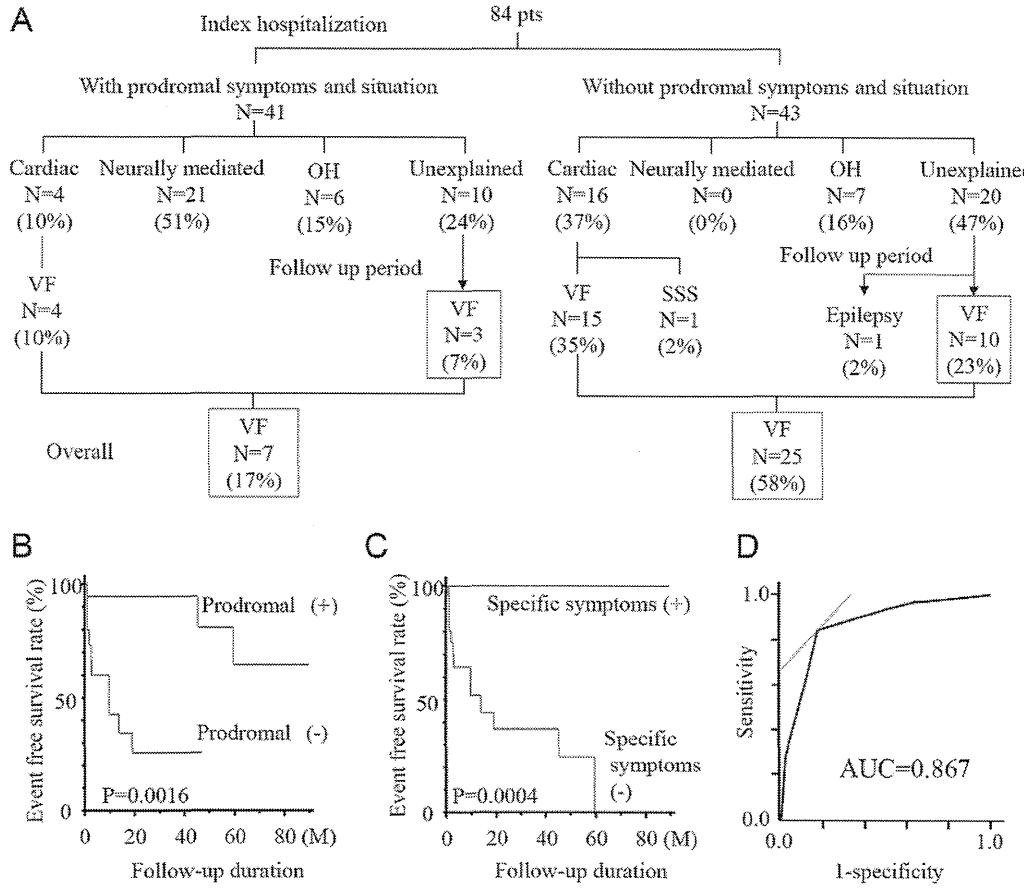


**Figure 2** Prognosis and risk factors for the occurrence of VF in patients with Brugada syndrome. **A:** Causes of syncope in Brugada syndrome patients with and without prodromal syndrome and situations at the initial visit and during the follow-up period. **B:** Freedom from lethal arrhythmic events for patients with and without prodromal symptoms and specific situations (blurred vision, relation to urination, diaphoresis, palpitations, and chest discomfort). Patients in the nonprodromal group often experienced recurrence of syncope owing to VF within 2 years from the first visit. **C:** Freedom from events for patients with and without existence of specific symptoms (blurred vision, diaphoresis, and relation to urination). Patients with specific symptoms did not suffer from VF during the follow-up period. **D:** Receiver-operating characteristic curve of the combination of fQRS, abnormal respiration, and absence of blurred vision. This combination was the highest AUC and had excellent accuracy of diagnosis for patients having VF. AUC = area under the curve; f-QRS = fragmented QRS; OH = orthostatic hypotension; SSS = sick sinus syndrome; VF = ventricular fibrillation.

## Discussion

### New observations

We found that syncope without prodrome was a high-risk sign associated with VF episodes. Although blurred vision, relation to urination, and diaphoresis were not associated with the occurrence of VF, 2 other prodromal symptoms—palpitations and chest discomfort—might be associated with VF episodes. We also found that syncope associated with VF often occurred in the supine position during sleep and was accompanied by convulsion and abnormal respiration. Therefore, absence of prodrome (especially blurred vision) and existence of abnormal respiration and f-QRS were important risk factors for the occurrence of VF in patients with BS and syncope. When syncopal episodes without documented VF at index hospitalization were accompanied by absence of blurred vision and existence of abnormal respiration and fQRS, VF was more likely in follow-up. Although vagal nerve activation can induce VF in patients with BS, patients did not have any vagally induced prodrome before the onset of VF.

### Syncope episodes in BS

Previous studies showed that spontaneous type 1 ECG and syncope episodes were predictors of arrhythmic events in patients with BS.[15,16] The FINGER study[17] showed that the cardiac event rate in patients with syncope was lower than that in patients with aborted sudden cardiac death but higher than that in asymptomatic patients. Thus, in previous studies, prognosis for patients with syncope was better than for patients with documented VF, although the syncope could have resulted from VF. This might be due to the fact that syncope episodes include both high-risk episodes related to VF and low-risk benign syncope episodes such as NMS and OH. Yokokawa et al[5] reported that one-third of the patients with BS had NMS, and they concluded that an impaired balance of the autonomic nervous system was related to their syncopal episodes. NMS[6] was also observed in asymptomatic patients with Brugada-type ECG. Thus, an indication for ICD implantation requires confirmation of the mechanism of syncope in patients with BS being benign or not. The HUT test is a useful tool for augmenting vagal

**Table 2** Characteristics of syncope in patients with and without prodromal symptoms

| Variables | Prodromal group | Nonprodromal group | *P* |
|---|---|---|---|
| Number of patients | 41 | 43 | |
| Symptom | | | |
| Syncope | 38 (93%) | 38 (88%) | NS |
| Faintness | 3 (7%) | 5 (12%) | NS |
| Prodromes | | | |
| Blurred vision | 28 (68%) | 0 (0%) | <.0001 |
| Relation to urination | 11 (27%) | 0 (0%) | .00018 |
| Diaphoresis | 10 (24%) | 0 (0%) | .00042 |
| Palpitation | 9 (22%) | 0 (0%) | .0009 |
| Chest discomfort | 6 (15%) | 0 (0%) | .0088 |
| Patients' condition after onset of syncope | | | |
| Convulsion | 6 (15%) | 10 (23%) | NS |
| Incontinence | 4 (10%) | 7 (16%) | NS |
| Falling down | 15 (37%) | 8 (19%) | NS |
| Any injury | 3 (7%) | 2 (5%) | NS |
| Abnormal respiration | 3 (7%) | 15 (35%) | .0018 |
| Position at the onset of syncope | | | |
| Supine | 3 (7%) | 18 (42%) | .0002 |
| Sitting | 15 (37%) | 12 (28%) | NS |
| Standing | 23 (56%) | 13 (30%) | .016 |
| Situation at the onset of syncope | | | |
| On exertion | 1 (2%) | 1 (2%) | NS |
| Standing-up | 7 (17%) | 7 (16%) | NS |
| Bathing | 4 (10%) | 2 (5%) | NS |
| Rest | 7 (17%) | 19 (44%) | .0068 |
| Sleeping | 3 (7%) | 15 (35%) | .0018 |
| Drinking | 4 (10%) | 6 (14%) | NS |
| Initial diagnosis of the syncope | | | |
| Arrhythmias | | | |
| VF | 4 (10%) | 15 (35%) | .0055 |
| SSS | 0 (0%) | 1 (2%) | NS |
| Neurally mediated syncope | 21 (51%) | 0 (0%) | <.001 |
| Orthostatic hypotension | 6 (15%) | 7 (16%) | NS |
| Unexplained | 10 (24%) | 20 (47%) | .035 |

Values represent n (%).

NS = nonsignificant; SSS = sick sinus syndrome; VF = ventricular fibrillation.

nerve activity and inducing NMS, but positive results of a HUT test in BS patients with syncope might incorrectly indicate syncope associated with VF as being benign vagal syncope.

Another dilemma related to autonomic nerve activation in BS is that vagal nerve stimulation could aggravate the pathophysiology of BS. Vagal nerve activation mediated by acetylcholine caused abbreviated epicardial action potential and augmented ST-segment elevation in ECGs in an experimental model of BS.[18] Heterogeneous loss of the phase 2 dome of the action potential initiates phase 2 reentry and polymorphic ventricular tachycardia. Infusion of acetylcholine into the coronary artery augmented ST-segment elevation without coronary vasospasm and induced VF.[8,19] Physiological conditions enhanced vagal nerve activity and also augmented ST-segment elevation in right precordial leads in relation to the occurrence of VF.[20]

Although prodrome was often accompanied by benign syncope[9,21] (such as NMS and OH), arrhythmic syncope had less prodromal symptoms.[22,23] It is difficult to differentiate benign syncope from ventricular tachyarrhythmia in patients with BS because vagal nerve activation can induce NMS as well as VF.[8,19] In the present study, we showed that patients did not have any vagally induced prodrome before the onset of VF. We analyzed prodrome and situations in detail and consequently found that syncope with blurred vision, diaphoresis, or a situation related to urination indicated benign symptoms mediated by NMS or OH in patients with BS. Palpitations and chest discomfort could be prodrome at the onset of VF.

**Table 3** Characteristics of syncope in patients without VF detection at index hospitalization between the prodromal group and the nonprodromal group

| Variables | Prodromal group | Nonprodromal group | *P* |
|---|---|---|---|
| Number of patients | 37 | 28 | |
| Symptom | | | |
| Syncope | 34 (92%) | 23 (82%) | NS |
| Faintness | 3 (8%) | 5 (18%) | NS |
| Prodromes | | | |
| Blurred vision | 26 (70%) | 0 (0%) | <.0001 |
| Relation to urination | 11 (30%) | 0 (0%) | .0060 |
| Diaphoresis | 10 (27%) | 0 (0%) | .0099 |
| Palpitation | 7 (19%) | 0 (0%) | .038 |
| Chest discomfort | 4 (11%) | 0 (0%) | NS |
| Patients' condition after onset of syncope | | | |
| Convulsion | 4 (11%) | 6 (21%) | NS |
| Incontinence | 4 (11%) | 6 (21%) | NS |
| Falling down | 14 (38%) | 4 (14%) | .0256 |
| Any injury | 3 (8%) | 2 (7%) | NS |
| Abnormal respiration | 3 (8%) | 6 (21%) | NS |
| Position at the onset of syncope | | | |
| Supine | 2 (5%) | 13 (46%) | .0002 |
| Sitting | 5 (18%) | 12 (32%) | NS |
| Standing | 23 (62%) | 10 (36%) | NS |
| Situation at the onset of syncope | | | |
| On exertion | 1 (3%) | 1 (4%) | NS |
| Standing-up | 7 (19%) | 7 (25%) | NS |
| Bathing | 3 (8%) | 1 (4%) | NS |
| Rest | 5 (14%) | 15 (54%) | .0001 |
| Sleeping | 2 (5%) | 11 (39%) | .0007 |
| Drinking | 3 (8%) | 4 (14%) | NS |
| Initial diagnosis of the syncope | | | |
| Arrhythmias | | | |
| VF | 0 (0%) | 0 (0%) | - |
| SSS | 0 (0%) | 1 (4%) | NS |
| Neurally mediated syncope | 21 (57%) | 0 (0%) | <.0001 |
| Orthostatic hypotension | 6 (16%) | 7 (25%) | NS |
| Unexplained | 10 (27%) | 20 (71%) | .014 |

Values represent n (%).

NS = nonsignificant; SSS = sick sinus syndrome; VF = ventricular fibrillation.